



IoT ready Eddy Current Testing Structural Health Monitor

Ana Margarida Sebastião Silvestre

Thesis to obtain the Master of Science Degree in

Electronics Engineering

Supervisor: Prof. Luís Filipe Soldado Granadeiro Rosado

Examination Committee

Chairperson: Prof. Pedro Miguel Pinto Ramos

Supervisor: Prof. Luís Filipe Soldado Granadeiro Rosado

Member of the Committee: Prof. Artur Fernando Delgado Lopes Ribeiro

October 2019

Declaração

Declaro que o presente documento é um trabalho original da minha autoria e que cumpre todos os requisitos do Código de Conduta e Boas Práticas da Universidade de Lisboa.

Declaration

I declare that this document is an original work of my own authorship and that it fulfills all the requirements of the Code of Conduct and Good Practices of the Universidade de Lisboa.

Acknowledgements

First of all, I would like to thank my supervisor, Professor Luis Filipe Soldado Granadeiro Rosado not only for the support, guidance and constant feedback through the elaboration of this dissertation, but also for the patience and time spent helping me in all situations.

A special thanks to Mr. Pina dos Santos for all the assistance in the hardware components development for this work. His availability and patience are reflected in the result of this dissertation and have been a constant throughout my entire academic path.

Here I end the path that started many years ago as a student and with it I take a lot of knowledge, life experiences, joyful moments and dreams to conquer.

I would then like to express my gratitude to my Master Thesis' cabinet colleagues for being always there to give advice and for all the fun moments during this journey.

To all my course mates with whom I worked during the course, especially the ones with whom I have shared a lot of hours solving and overcoming the challenges our course imposed us;

Finally, a special thanks to the most important people in my life: (1) my parents, for always pushing me forward during my entire academic course and for investing financially in my future; (2) my grandparents, that always cared about me and took care of me since I was a baby; (3) to my boyfriend, that has always been there for me, supporting me in all my life decisions and encouraging me for doing what I wanted; (4) my best friends, for all the patience during the more stressful moments and for always being there for me during this journey that ends with this dissertation.

Abstract

Non-destructive testing is used to ensure and evaluate the quality of a product or material while detecting defects, without causing any damage. Eddy current testing is an electromagnetic and non-destructive method used to identify and assess surface, or near-surface, defects on materials and structures, through detecting discontinuities in segments that conduct electricity. Structural Health Monitoring is one application of non-destructive testing, being a set of systems that gives a continuous and periodic diagnostic of a structure. The method determines and analyzes all defects in the structure to provide preventive support and avoid a collapse. To turn this in real-time monitorization, a platform that supports all remote access to sensorial data and physical devices is being used, named Internet of Things.

This work uses a designed electronic system that implements eddy current testing in a structural health monitoring system. It reads multiple probes, saves the data collected and evaluates it. The system uses the ESP32 microcontroller to process the information collected through all sensors. It also connects through a Bluetooth connection with a computer allowing real-time evaluation. The device is hardware ready for communications using Narrowband-IoT Low-Power Wide Area Network, and to report alarms previously deliberated to the cloud. The host can control the device and evaluates the results from it with a Graphical User Interface. If required the device works in an autonomous mode, programming the readout channels with the last saved configuration. The system was tested with a setup to monitor the crack growing.

Keywords

Non-Destructive Testing, Structural Health Monitoring, Eddy Current Testing and Internet of Things.

Resumo

O ensaio não destrutivo usa-se para garantir e avaliar a qualidade de um produto ou material, detetando faltas sem causar danos. O ensaio por correntes induzidas é um método eletromagnético sem contacto usado para identificar e avaliar falhas numa superfície, ou perto desta, em materiais e estruturas, detetando descontinuidades em secções condutoras de eletricidade. A monitorização da integridade estrutural faz parte das técnicas de avaliação não destrutivas, sendo um conjunto de sistemas que diagnosticam continuamente e periodicamente o estado da estrutura. O método identifica e analisa os defeitos na estrutura, apoiando-a preventivamente e evitando um colapso. Para garantir uma monitorização em tempo real, a plataforma “Internet das Coisas” que suporta o acesso remoto a dados sensoriais e dispositivos físicos é utilizada.

Este trabalho usa um sistema eletrónico que implementa o ensaio por correntes induzidas num sistema de monitorização da integridade estrutural. O sistema lê várias sondas, recolhe os dados e avalia-os. Este usa o microcontrolador ESP32 para processar a informação recolhida pelos sensores e conecta-se através de Bluetooth a um computador, permitindo a avaliação em tempo real. O dispositivo está preparado em hardware para comunicações através da rede “Low-Power Wide Area Network Narrowband”, e para reportar alarmes previamente deliberados a uma plataforma na “cloud”. O controlo do dispositivo e avaliação de resultados é feito através de uma interface gráfica. O dispositivo pode trabalhar em modo autónomo, programando-se os canais de saída com a última configuração guardada. O sistema foi testado com um “setup” para monitorizar o crescimento da falha.

Palavras-chave

Ensaio Não Destrutivo, Ensaio por Correntes Induzidas, Monitorização da Integridade Estrutural e Internet das Coisas

Contents

- Acknowledgements V
- Abstract VII
- Keywords..... VII
- Resumo IX
- Palavras-chave..... IX
- List of TablesXV
- List of FiguresXV
- List of Acronyms XVIII
- Chapter 1 - Introduction 1
 - 1.1. Purpose and motivation 1
 - 1.2. Goals and challenges 2
 - 1.3. Document Organization 2
- Chapter 2 - State of the Art 5
 - 2.1. Non-destructive testing 5
 - 2.1.1. Radiography 5
 - 2.1.2. Magnetic particle crack detection 6
 - 2.1.3. Dye penetrant testing 7
 - 2.1.4. Ultrasonic Flaw Detection 8
 - 2.2. Eddy Currents 9
 - 2.2.1. Eddy currents phenomenon 9
 - 2.2.2. Depth of penetration 10
 - 2.2.3. Eddy Currents Probes 11
 - 2.2.4. Probe excitation techniques 14

2.2.5. Eddy Current Inspection	14
2.2.6. Research and application	15
2.3. Structural Health Monitoring	16
2.3.1. Structural Health Monitoring Categories	16
2.3.2. Structural Health Monitoring Module	18
2.3.3. Research and application	18
2.4. Internet of Things.....	19
2.4.1. Internet of Things organization	19
2.4.2. Advantages and disadvantages.....	21
2.4.3. Research and application	21
2.5. Related work.....	21
Chapter 3 -Hardware.....	24
3.1. Processor.....	25
3.2. Power management	27
3.3. Environment sensors	28
3.4. Eddy Current Testing.....	29
3.5. Narrowband-IoT.....	31
3.6. Printed Circuit Board	32
Chapter 4 - Firmware and Software	34
4.1. Communication protocol.....	34
4.1.1. Protocol description	34
4.1.2. Commands explanation	35
4.2. Peripherals readout	36
4.2.1. I2C interface.....	36
4.2.2. Temperature and Humidity sensor	37
4.2.3. Acceleration sensor	38
4.2.4. Inductance-Digital Converter	38
4.3. Code organization	41
4.4. Graphical User Interface.....	42
4.5. Main execution flow	45
Chapter 5 - System description and measurements.....	47

5.1. Setup	47
5.1.1. Probes.....	48
5.1.2. Structure.....	48
5.2. Data acquisition	49
5.3. Production cost.....	50
Chapter 6 - Conclusion.....	53
6.1. Summary and Achievements.....	53
6.2. Future Work.....	54
References	56
Appendix I - Commands definition	61
Appendix II – PCB design	64

List of Tables

- Table 2.1 - SHM categories. 17
- Table 2.2 - SHM techniques comparison. 19
- Table 2.3 - Wireless protocols. 20
- Table 4.1 - Commands description. 34
- Table 4.2 - Commands definition example. 36
- Table 4.3 - Command description of Si7021. 37
- Table 4.4 - Commands description of LIS2DE12. 38
- Table 4.5 - Commands description of LDC1614. 40
- Table 5.1 - Coils values. 48
- Table 5.2 - Production cost. 51

List of Figures

- Figure 2.1 - Radiography method [1]. 6
- Figure 2.2 - Magnetic particle testing method [1]. 7
- Figure 2.3 - Dye penetrant testing method [1]. 7
- Figure 2.4 - Ultrasonic detection method [1]. 8
- Figure 2.5 - Eddy Current phenomenon [11]. 10
- Figure 2.6 - Eddy current standard depth of penetration [13]. 11
- Figure 2.7 - Absolute probe electric circuit. 12
- Figure 2.8 - Differential probe electric circuit. 12
- Figure 2.9 - Reflection probe electric circuit. 13
- Figure 2.10 - Hybrid probe electric circuit. 13
- Figure 2.11 - Change of the coil induced voltage due to a crack [14]. 14
- Figure 2.12 - Benefits of including SHM [21]. 16
- Figure 2.13 - Principle and organization of a SHM system [21]. 18
- Figure 2.14 - IoT organization [37]. 20

Figure 3.1 - System architecture.	24
Figure 3.2 - Functional block diagram of ESP32 [47].	25
Figure 3.3 - ESP32 Evaluation Board.	26
Figure 3.4 – Power management circuit.	28
Figure 3.5 – Functional block diagram [48].	28
Figure 3.6 – Block diagram [49].	29
Figure 3.7 – Simplified integration of the LDC1612 with an MCU [50].	30
Figure 3.8 – Detailed block diagram of LDC1614 [50].	31
Figure 3.9 - Main Board PCB top layer (a) and bottom layer (b)	32
Figure 4.1 - Command structure.	35
Figure 4.2 - I ² C Interface buses.	36
Figure 4.3 - LDC1614 configuration structure,	41
Figure 4.4 - Command definition tab.	43
Figure 4.5 - Data acquisition tab.	43
Figure 4.6 – Autonomous mode tab.	44
Figure 4.7 - Environment data tab.	44
Figure 4.8 - Main execution flow chart.	45
Figure 5.1 - ECT setup.	47
Figure 5.2 - Measurements over distance through four channels, perpendicular cracks.	49
Figure 5.3 - Measurements over distance through Channel 0, perpendicular cracks.	50
Figure 5.4 - Data acquisition over distance, longitudinal crack.	50

List of Acronyms

3GPP	<i>Third Generation Partnership Project</i>
°C	<i>Degrees Celsius</i>
AC	<i>Alternating Current</i>
ACK	<i>Acknowledge</i>
ADC	<i>Analog to Digital Converter</i>
AE	<i>Acoustic Emission</i>
CPU	<i>Central Processing Unit</i>
CS	<i>Chip Select</i>
ECT	<i>Eddy Current Testing</i>
eDRX	<i>External Discontinuous Reception</i>
EM	<i>Electromagnetic</i>
EMAT	<i>Electromagnetic Acoustic Transducer</i>
FFT	<i>Fast Fourier Transform</i>
GMR	<i>Giant Magneto-resistive</i>
GPIO	<i>General Purpose Input/Output</i>
GUI	<i>Graphical User Interface</i>
H	<i>Henry</i>
I²C	<i>Inter-Integrated Circuit</i>

ICs	<i>Integrated Circuits</i>
IDE	<i>Integrated Development Environment</i>
IoT	<i>Internet of Things</i>
LDC	<i>Inductance-to-Digital Converter</i>
LDC1614EVM	<i>LDC1614 Evaluation Module</i>
LDO	<i>Low-dropout</i>
LGA	<i>Long Grid Array</i>
LPWAW	<i>Low-Power Wide Area Network</i>
LSb	<i>Least Significant bit</i>
LTE	<i>Long Term Evolution</i>
MCU	<i>Microcontroller Unit</i>
MEMS	<i>Micro Electro-Mechanical System</i>
NACK	<i>No Acknowledge</i>
NZIF	<i>Near Zero Intermediate Frequency</i>
NB-IoT	<i>Narrowband-IoT</i>
NDT	<i>Non-Destructive Testing</i>
PCB	<i>Printed Circuit Board</i>
PSM	<i>Power Saving Mode</i>
RFID	<i>Radio Frequency Identification</i>
RTC	<i>Real-Time Clock</i>
SCL	<i>Serial Clock</i>
SDA	<i>Serial Data</i>
SHM	<i>Structural Health Monitoring</i>

SI	<i>System of Unit</i>
SRAM	<i>Static Random Access Memory</i>
SPP	<i>Serial Port Protocol</i>
UE	<i>User Equipment</i>
VM	<i>Virtual Machine</i>

Chapter 1 - Introduction

1.1. Purpose and motivation

Non-destructive Testing (NDT) is the principal method for inspection used in metallic parts and welding joints. This procedure is due to its viability and capability of not changing the product that is being inspected, saving money and time in evaluation, damage assessment and research. NDT is used in aerospace, automotive, chemical, nautical and industrial applications. Some types of NDT methods are radiography, magnetic particle crack detection, dye penetrant testing, ultrasonic flaw detection and eddy currents and electro-magnetic testing [1].

Eddy Current Testing (ECT) is an electromagnetic and non-contact method used to identify and assess surface breaking or near surface defects on materials and structures, through detection of discontinuities in segments that conduct electricity. Eddy currents, also known as Foucault currents, are electrical currents induced when a conductor experiences a change in the intensity or direction of a magnetic field. Whenever these currents interact with an obstacle, for example a crack, the current in the vicinity becomes distorted.

Structural Health Monitoring (SHM) is expanding as improving and nowadays it is essential, not only to monitor and maintain structures, but also to preserve infrastructures and buildings' integrity, with the goal of ensuring the safety of human beings. SHM makes part of a group of nondestructive evaluation techniques used to monitor the security of structures, which brings benefits such as improving safety standards, detecting early reliability risks, longer structural life spans and reducing costs. All this means that promoting SHM will, in the end, also promote overall public protection. To accomplish this improvement there are new guidelines and policies to ensure safety building and construction, as well as new technologies that facilitate security control, such as instrument supervising and testing of digital information about infrastructures security that are being studied. The advances in SHM, like the use of sensors, collection of data on demand and its analysis, promote engineers' capacity of contributing to public safety, which has a key importance with a growing number of aging structures. One of the advantages of these advances in SHM is the ability of helping professionals to detect potential risks to a structure safety, for example damages provoked by failed pipelines and other structures that transport water (e.g. in dams), through the use of sensors that monitor the modifications in water levels and are able to detect earlier leaks in infrastructures. Other example is the ability to identify ground movement, such as earthquakes and other disasters, preventing or diminishing huge structural risks created by

them. One consequence of the frequent monitorization and maintenance on structures and buildings, by installing sensors and complement technology that provides details relatively to the health of a structure, is an increase of their life span. With the progress of technology, new methods also provide more accuracy and reliability on data collection and analysis. SHM creates a real-time analytical method that itself also allows more accuracy in monitorization and risk analysis. Cost efficiency is, as well, an important reason that justifies its use as with improved maintenance of the buildings, the number of infrastructures that will suffer demolition and expensive massive rebuilding are smaller.

Internet of Things (IoT) refers to a concept of a diversity of objects, such as sensors, mobile phones, radio-frequency identification (RFID), etc. These objects are capable to interconnect with each other, and, because of that, create an enormous network where all items are connected through the Internet. In this way, it is possible to complete information transmission, plan and process to allow systems to identify, locate and monitor objects in real time. Combining SHM with IoT permit the collection of critical structural health specifications with rapid response, off-loading computational power, store data, and remotely monitoring.

1.2. Goals and challenges

The main objective of this work is to make a device capable of implementing ECT in a SHM approach, which can be installed and operate in an autonomous and permanent way while monitoring a structure. This system must be able of read multiple eddy current sensors, save the measurements and then analyze them. If needed, the system will generate alarmistic concerning the presence or growth of the monitored fault. It also must contain a wireless link to complete an interconnection with a computer, granting the collection of preserved data and real-time operation/monitorization. The utilization of a Low-Power Wide Area Network (LPWAN) type communication, in particular Narrowband-IoT (NB-IoT), will allow the device to report the alarms previously deliberated directly to the cloud. As such, the goals set for this project are:

- Find front-end circuits for eddy currents that fit the situation of permanent installation with acceptable cost;
- Program an interface between an embedded processing core and the host processor and the circuits referred before;
- Develop firmware for collection, storage and interpretation of signals;
- Develop the Interface between a chosen NB-IoT communication module and the embedded processing core;
- Program the communication between the graphic interface and the computer.

1.3. Document Organization

This document is composed of four chapters, whose content is now briefly described.

Chapter 2 begins with a description of some NDT techniques being the main focus ECT explanation and inspection techniques, enumerating and describing the different existents probes. Then SHM systems functionality are summarized. To finish, the use of IoT and the benefits of its integration with SHM are described.

Chapter 3 is reserved to the all explanation of the hardware implemented in the project, containing also the description of the system's architecture and requirements of the system.

Chapter 4 has divided into the peripherals and the communication with the host. Both of them are firmware and software description and explanation.

Chapter 5 is reserved to the explication of the setup build to follow the test structure and the results collected from the probe.

Chapter 6 describes the conclusions of the work.

Chapter 2 - State of the Art

2.1. Non-destructive testing

Although there is not a settled starting date, NDT has been used for many years. The first dated case was in 1868 when S. H. Saxby used the magnetic characteristics of a compass to detect cracks in gun barrels. The evolution of NDT techniques became more important and necessary since World War II, when modern industry emerged, due to the necessity of having more testing equipment and to produce flawless components. From then on, these have been developed and improved over the years [2].

NDT is a set of non-invasive inspection techniques which purpose consists on analyzing material properties, components and even entirely processed units in a safe, trustworthy and cost-effective way without causing damage. The functionality of these techniques involves also the detection, characterization and/or measurement of damage mechanisms presence. Some NDT techniques can locate defects and determine the features of the detected defect.

The more common NDT methods used in industry are radiography, magnetic particle crack detection, dye penetrant testing, ultrasonic flaw detection, eddy currents and electro-magnetic testing. Radiography is a technique suitable for the discovery of internal defects in ferrous and non-ferrous metals [3] and magnetic particle crack detection is suitable for the detection of discontinuities in magnetic materials [4]. On the other hand, the dye penetrant testing is used to determine the surface-breaking flaws in non-ferromagnetic materials [5] and the ultrasonic flaw detection is used for the discovery of defects in sound conducting materials [6]. Finally, the eddy current testing is used for detecting flaws, conductivity measuring and coating thickness measuring [7].

2.1.1. Radiography

Radiography technique is based in X-rays and gamma rays, being the difference between them wavelengths in their origin. X-rays are generated by an x-ray generator and gamma rays are emitted by radio-active isotopes. Both types of radiations are part of the electromagnetic spectrum. As they have no charge and no mass, they are not influenced by electrical and magnetic fields and, usually, travel in straight lines. Radiations are differentially absorbed by the material through the way it passes. The greater the thickness and the denser the material is, greater the absorption [8].

In X or Gamma radiography the film package, which is the junction of film and intensifying screens confined in a light tight cassette, is placed proximally to the surface of the object. The radiation source is fixed with some distance of the object and, after that, the radiation passes straight through the object heading directly to the film. When the time of exposure ends, the film is removed, processed, dried and can be seen with light on a special viewer. This process is shown in Figure 2.1.

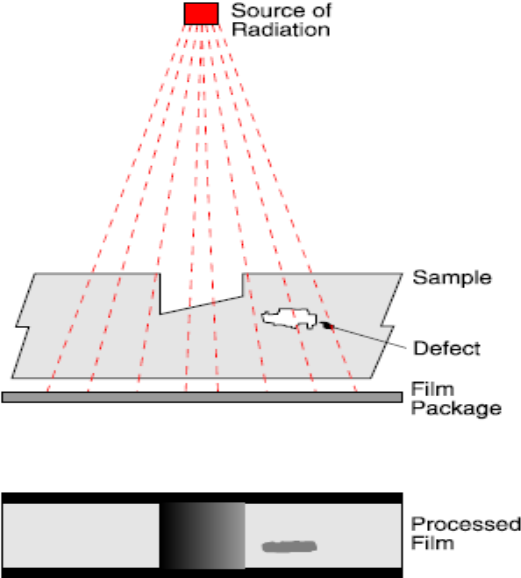


Figure 2.1 - Radiography method [1].

Some advantages of radiography are the utility in thin sections, the applicability in any material and the fact that information is presented pictorially. In the disadvantages list of this technique are included the possibility of provoking health hazard, the non-application on finding surface defects and the non-indication of depth in a defect below the surface.

2.1.2. Magnetic particle crack detection

Magnetic particle testing uses magnetized ferromagnetic material, due the existence of a discontinuity, being a leakage magnetic field generated by the workpiece surface and near-surface magnetic-curve. This leakage magnetic field is able to absorb magnetic particles on the workpiece surface and create visible indications in right light, thus identifying the location, shape, size and severity of the discontinuity [4].

A schematic for detecting longitudinal defects using current flow which passes through the subject is shown in Figure 2.2 (a). A schematic of an encircling coil with the aim of detecting circumferential and transverse defects is represented in Figure 2.2 (b).

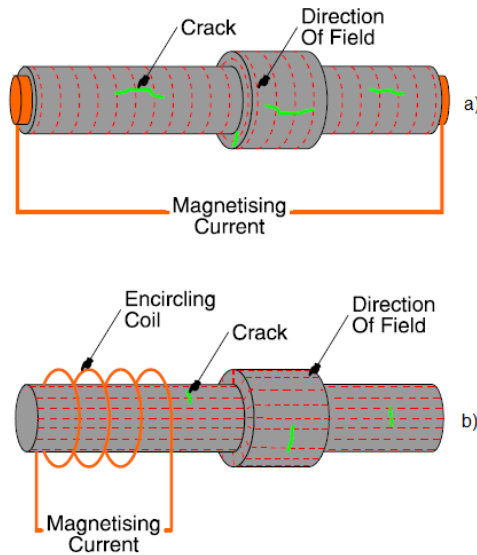


Figure 2.2 - Magnetic particle testing method [1].

Magnetic particle testing has some advantages such as high simplicity of operation and application, and the fact that it is a quantitative method and can be automated. However, this NDT method has also disadvantages like being only applicable to ferromagnetic materials and to surface or near surface flaws.

2.1.3. Dye penetrant testing

Dye penetrant testing requires the cleaning of the part being analyzed with a strong solvent and then immerse that part in the penetrant in a period around the tenths of minutes. After that, the surplus penetrant is removed with a strong solvent and is applied a thin coating of chalk. A period of time afterwards, the chalk draws the dye out of the crack.

The process is illustrated in Figure 2.3 labeled with the respective part of the sequence.

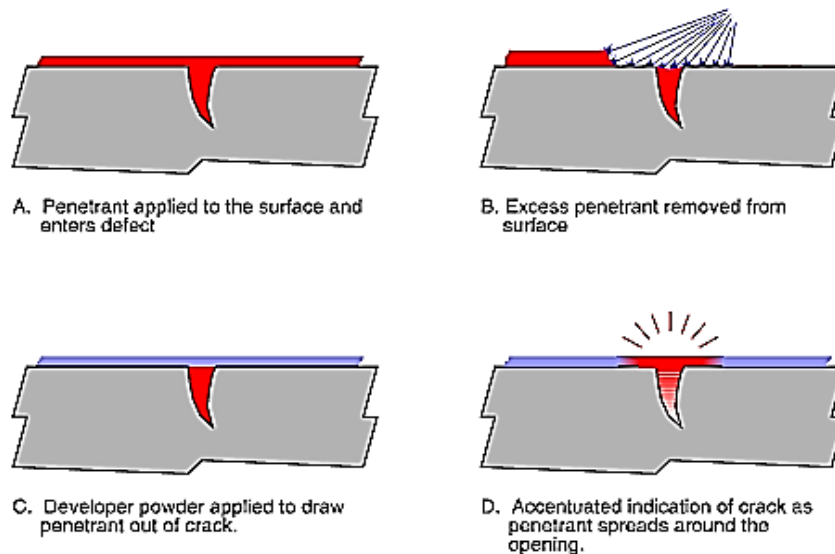


Figure 2.3 - Dye penetrant testing method [1].

Dye penetrant testing has some advantages such as being one of the best methods created for surface breaking cracks in non-ferrous metals, being a quantitative method and having simplicity in the operating mode. Nevertheless, this technique has decreased sensitivity, uses very consumables and has restrictions to surface breaking defects.

2.1.4. Ultrasonic Flaw Detection

Ultrasonic detection technique is based in using sound waves which have frequency in the range of MHz. There are two different methods in this technique: pulse-echo and through transmission. The former method used only one transducer and the more recent one uses two. A pulse of mechanical energy is transmitted inside the component by the piezoelectric material and this energy goes through the material, reflecting from the back surface being detected by the same transducer, generating a signal shown in an oscilloscope. The capture is composed by the original pulse of the ultrasonic transducer, the back reflection and also a reflection from a found defect through a blip. The depth of the defect below the surface is determined through oscilloscope timing. In the transmission method, transducers are fixed on opposite sides of the component being analyzed and when there is a decrease of intensity sensed by the receiving transducer, it indicates the defect shadowing part of the ultrasonic radiation [9].

This technique can identify cracks oriented in the plane of and normal to the surface of components using normal or angle beams. The ultrasonic detection technique is described in Figure 2.4, where Figure 2.4 (a) uses a normal beam and Figure 2.4 (b) uses an angle beam.

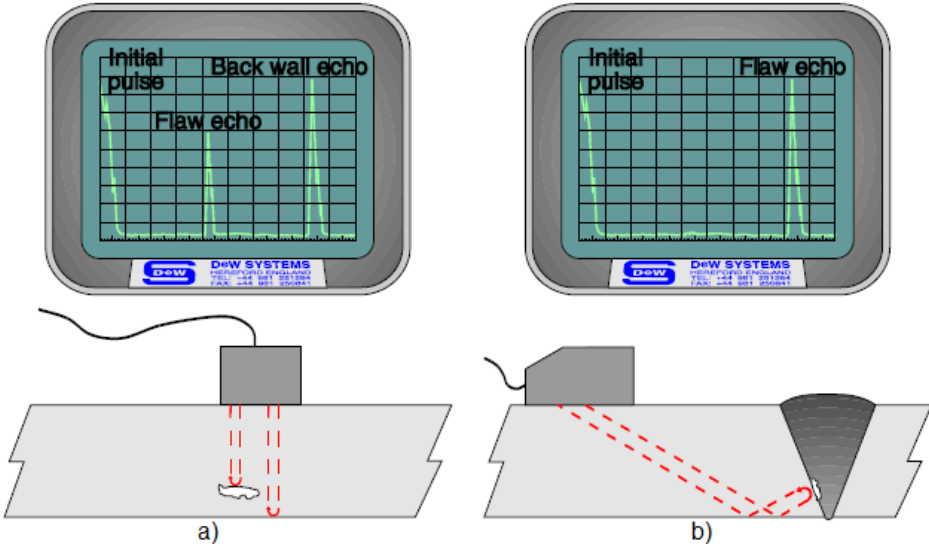


Figure 2.4 - Ultrasonic detection method [1].

The ultrasonic technique has multiple advantages such as having instant test results, being able to determine position, size and type of the defect, and being portable. However, this technique has also some disadvantages like being impossible to save permanent record unless it uses sophisticated data collection systems, needing interpretation of indications and having difficulties in analyzing thin sections.

2.2. Eddy Currents

The scientist who was credited for discovering eddy currents was the French Jean Foucault, in 1855, by building a device that used a copper disk moving in a strong magnetic field showing that eddy currents' generation is due to a moving object within a continuous magnetic field. The testing using eddy currents began after 1831, when the English scientist Michael Faraday discovered electromagnetic induction. Faraday realized that an electric current would flow through a conductor (a material in which electrons move easily) when a magnetic field passed through a conductor or the opposite process, but only if there is a closed path through which the current could circulate [10]. This phenomenon was only used for the first time in 1879. The English scientist David Hughes illustrated in what way the properties of a coil change when placed within metals of different magnetic permeability and conductivity, which allowed comparison and sorting of different materials. Nevertheless, only since World War II eddy currents were applied for material testing.

Nowadays, thanks to the technological progress there was a great evolution in non-destructive techniques, in particular eddy current testing [11], being this type of non-destructive technique widely used performing quality controls tests. The major advances contributed to the development of eddy current testing were the evolution of micro and nano-electronics field, as it was made possible to build microprocessors with many power, reduced cost and high precision analog to digital converters. As result, it is possible to make real-time processing in portable battery-powered devices which can show resultant information to a user through a display [12].

2.2.1. Eddy currents phenomenon

Faraday's induction law and Ampère's law are the base of eddy currents phenomenon. As stated with Ampère's law, the integral around a closed path S of the component of the magnetic field B tangent to the direction of the path is

$$\oint_S \vec{B} \cdot d\vec{S} = \mu I , \quad (2.1)$$

where μ is the permeability of the medium and I is the electric current that flows through the surface bounded by the closed path. Through (2.1), it is possible to determine the magnitude of the magnetic field formed around a wire in a direction perpendicular to the one of the flowing currents, knowing the distance r from it, by

$$B = \frac{\mu I}{2\pi r} . \quad (2.2)$$

According to Faraday's law, when a magnetic flux through a surface bounded by a wire (a conducting path) has some change, a non-electrostatic electric field is induced and being equal to the electromotive force induced in the wire with a magnitude equal to the rate of change of the flux, as proved in

$$\varepsilon = \oint_c \vec{E} \cdot d\vec{l} = -\frac{d\Phi_B}{dt} , \quad (2.3)$$

where

$$\Phi_B = \int \vec{B} \cdot d\vec{A} . \quad (2.4)$$

Conventional eddy currents technology uses a probe comprised by a coil that, when excited with an alternating current, creates a magnetic field (in blue) represented in Figure 2.5 (a). When the coil is positioned over a conductive part, it is created opposite alternating currents, Figure 2.5 (b) (red), named by eddy currents. Moving the coil over the homogeneous material, the impedance value of the coil remains constant, however if there is a defect in the material the path of eddy currents is disturbed (in yellow) (Figure 2.5 (c)) and the magnetic field created is less intense. In result, with the variation of electric impedance in the probe it allows the defect detention.

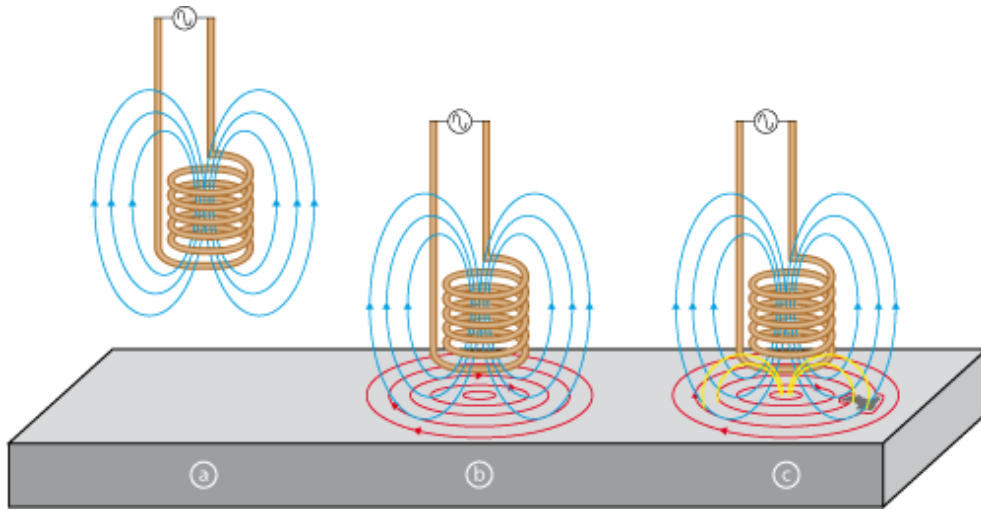


Figure 2.5 - Eddy Current phenomenon [11].

2.2.2. Depth of penetration

Eddy currents flow is not equally distributed along the test material depth. It has its maximum intensity at the conductor surface and it decreases as depth increases. This phenomenon is called skin effect and, as a result, the capability of detecting buried defects is limited. The current density at depth x is

$$J(x) = J_0 e^{-x\sqrt{\pi f \mu_0 \mu_r \sigma}} , \quad (2.5)$$

where J_0 is the maximum value of current density at conductor surface which corresponds to $x = 0$.

The value is null if the operation frequency f is also null and it increases as frequency value rises.

μ_0 corresponds to the magnetic permeability of free space, μ_r is the relative magnetic permeability of the material and σ refers to electric conductivity of the material in test.

To quantify the depth of detection, the so-called standard depth of penetration is used, this translates the depth at $1/e$ ($\approx 36.7\%$) of the current value measured at the conductor's surface. The standard depth of penetration is shown by Figure 2.6 and expressed in

$$\delta = \frac{1}{\sqrt{\pi f \sigma \mu}} , \quad (2.6)$$

where δ is the standard depth of penetration, f is the excitation signal frequency, σ is the electrical conductivity of the material, and μ is the magnetic permeability of the material. In (2.6) is demonstrated that the standard depth of penetration decreases with the increase of the excitation signal frequency, maintaining the electrical conductivity and the magnetic permeability constant.

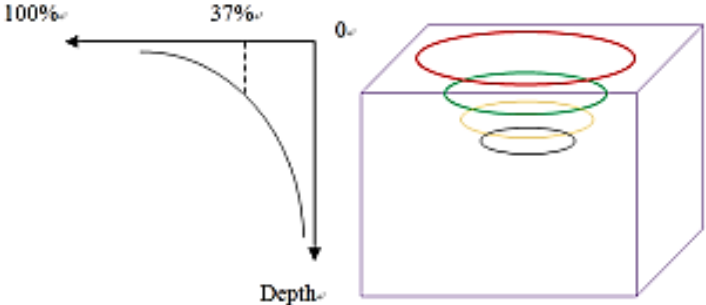


Figure 2.6 - Eddy current standard depth of penetration [13].

2.2.3. Eddy Currents Probes

To test with an eddy current instrument a given piece, an eddy current probe is needed. An important issue with this subject is that there are different types of probes, which can be custom made to best suit their function and/or application. This allows eddy current probes to be classified by configuration and mode of operation of the test coils. Configuration of a probe usually refers to how a coil or coils are connected to best couple testing material. In the other hand, the mode of operation indicates how the coil or coils are wired and integrated with the test equipment. The mode of operation of a probe is normally inserted in one of four categories described below:

2.2.3.1. Absolute Probes

This type of probes is also known as single-coil probes, as their composition is based in a single test coil which aims to generate eddy currents and perceive changes in the eddy current field.

The operating mode is described as an alternating current crossing the coil and generating a magnetic field, and when approaching the coil near a conductive material the magnetic field creates eddy currents. Its generation takes energy from the coil that results in the increase of the coil's electrical resistance. A magnetic field is generated by eddy currents being opposed to the one created by the coil and changes the inductive resistance of the coil. To detect a change in the testing material, the coil's impedance must be measured and analyzed. The electric circuit of this type of probe is in Figure 2.7.

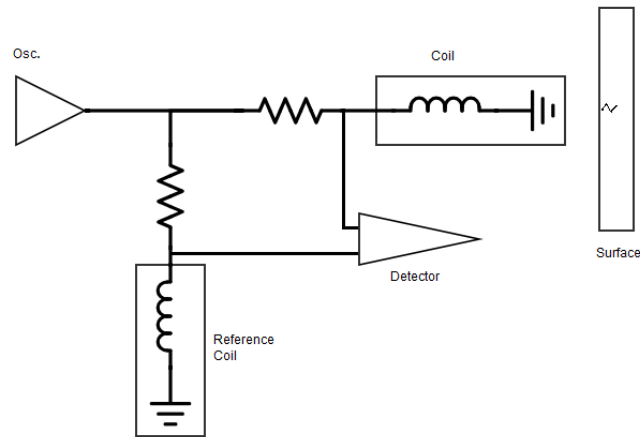


Figure 2.7 - Absolute probe electric circuit.

Absolute probes have various applications such as flaw detection, conductivity measurements, lift-off measurements and thickness measurements. Although they have a lot of versatility, they are also sensitive to conductivity, permeability liftoff and temperature. To improve the exploration range, it is included a second reference coil which is not in contact with the material surface.

2.2.3.2. Differential Probes

Differential probes are composed by two active coils that can be wound in opposition or in phase. When both coils are over a zone with no defects there are no differential signal generated between these coils. Nevertheless, when one of the coils is over a flaw and the other is over a non-defected zone, a differential signal is generated. The electric circuit that represent differential probes is shown in Figure 2.8.

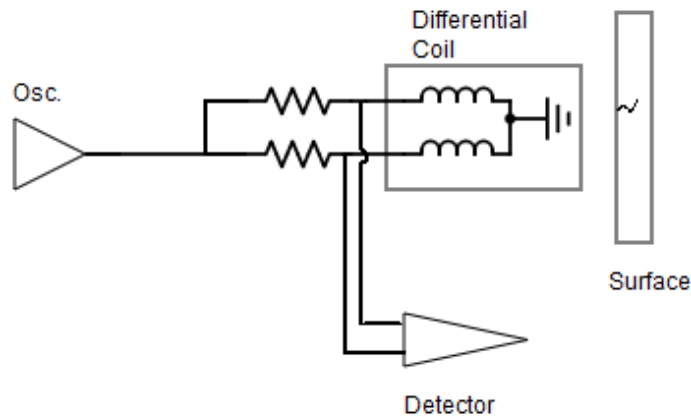


Figure 2.8 - Differential probe electric circuit.

Although they have high sensitivity to defects, there is some insensitivity to other properties that vary slowly. Other characteristic is the probe wobble signals are reduced. However, differential probes also contain one disadvantage related to the difficulties of interpreting the signals. This happens, for example, due to the size of a flaw being longer than the spacing between the two coils, which results in the detection of only the leading and trailing edges of the flaw.

2.2.3.3. Reflection Probes

Reflection probes are, like differential probes, constituted by two coils, but in this case one of the coils is used to excite the eddy currents and the other has the goal of sensing changes in the testing material. These are usually named driver/pickup probes. The electric circuit of reflection probes is represented in Figure 2.9.

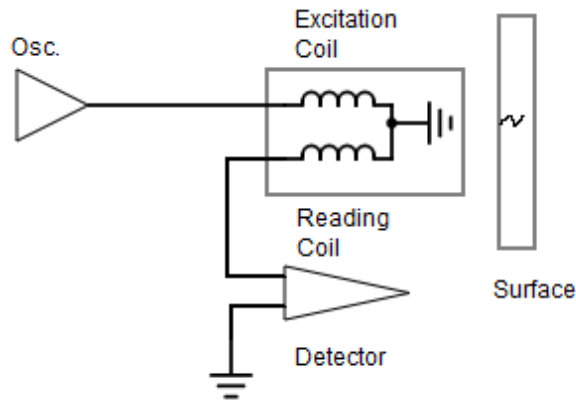


Figure 2.9 - Reflection probe electric circuit.

A benefit of these probes is the possibility of driver and pickup coils being optimized separately for each of their purposes.

2.2.3.4. Hybrid Probes

Hybrid probes usually have a stimulation coil, whose objective is to create an alternating magnetic field and other magnetic sensing elements. The electric circuit that corresponds this probe is represented in Figure 2.10.

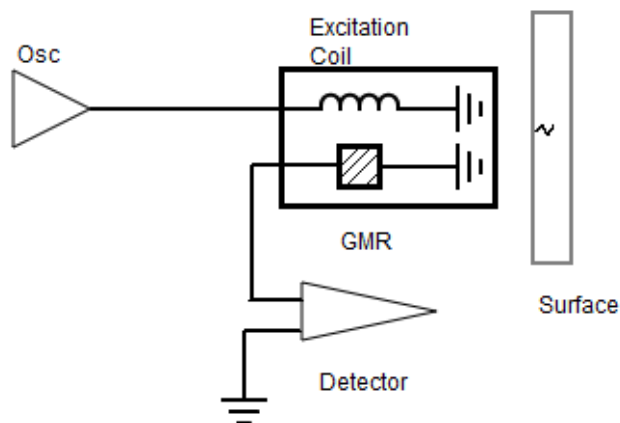


Figure 2.10 - Hybrid probe electric circuit.

There are many examples of these probes such as split D which has a driver coil that circles two D shaped sensing coils and works both in reflection mode or differential mode. Other example is one that through a conventional coil generates eddy currents in the material and then uses a distinct type of

sensor to discover changes in the test sample. To finish, another example is detecting changes in the magnetic flux through Hall effect sensor.

2.2.4. Probe excitation techniques

The use of single frequency techniques is not the only technique available for eddy current testing. There is a method that is based in harmonic excitation which characteristics are the application of discrete frequencies, larges dynamic range, accurate flaw sizing, high speed and signal analysis by pattern recognition [4]. In a presence of a defect in the tested material, the amplitude and phase of the electromagnetic field change implying changes, leading to a change in the coil induced voltage as shown in Figure 2.11.

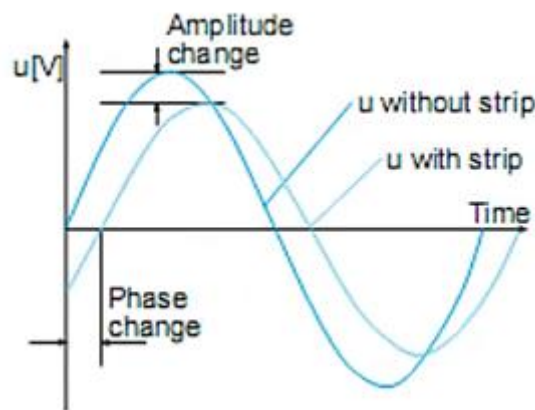


Figure 2.11 - Change of the coil induced voltage due to a crack [14].

Other type of excitation technique is multiple frequency eddy currents techniques that can be expressed by the generation of an eddy currents probe excitation signal with multiple frequency components and receive the probe response in a single test. This technique has some advantages such as decreasing inspection time by testing with different frequencies, improving sensitivity to different types of discontinuities and easily interpreting complex signals [15].

Pulsed eddy current techniques use a periodic pulse, with a duty cycle lower than 50%, to excite the probe. Through modulation of the pulse signal, it is allowed to, at the same time, test multiple frequency component. Some advantages of this method are the decrease of power consumption and the ability of being more robust to interference [16].

2.2.5. Eddy Current Inspection

2.2.5.1. Advantages

Although NDT includes multiple sensing technologies besides ECT, this method has advantages compared to the others existing. Eddy current sensors have high sensitivity to detect small flaws and defects in the surface or near it and in a determinate range, it is possible with good linearity indication. These sensors can also detect defects through non-conductive surface coating in excess of 5 mm

thickness. Inspections using these sensors are obtained almost instantly and the equipment need is portable. To finish, these sensors allow the analyze of the material with no contact with it.

2.2.5.2. Limitations

The principal limitation of this method is the need of the tested material being conductive and the necessity of the sensor being closed to the surface due to the eddy currents limitation of only existing on the surface and near surface. The surface in test needs to be polished to avoid interferences to accomplish a correct analysis, and the depth of the measure is limited. Other limitation of eddy current sensors is the high susceptibility to magnetic permeability, this means that a small change in permeability results in a huge effect in eddy current.

The geometry of the material may be a problem in inspection, a probe not being coupled perpendicularly at the material surface shows an electric impedance variation named lift-off. If the defect to be detected has a size or morphology hard to detect, this impedance variation due to lift-off may be superior to the impedance variation caused by that defect. This means that the signal cause by the defect is absorbed by the lift-off noise, which not allows the location and sizing of defect.

2.2.6. Research and application

The interest in eddy currents, along the years, has been raising specially in NDT industrial applications, medical applications and, the type of applications that is this works, structural health monitoring. This technique is used worldwide in different applications besides the crack detection, tube and wire testing, and condenser tube inspection implemented in SHM systems, as it is also used to material sorting, weld testing, coating thickness measurement, vibration and position sensing.

In [17], the use of eddy currents to inspect metallic aircraft components is presented, particularly to detect surface cracks and also corrosion damage. It still enumerates the main advantages and disadvantages of this method to this application. The paper [7], also describes the application of eddy currents to monitoring in aircraft application, along with fatigue testing.

As referred previously, eddy currents can be used in tube inspection [18]. In this case they used a sine wave generator circuit, two amplifier circuit, a voltage controlled current source, a filter circuit, two detector circuits, a comparator circuit, a display circuit and an eddy current probe.

Electrical conductivity of a metal relies on different factors, like its chemical composition and stress state of its crystalline structure. Measure electrical conductivity is possible through eddy current techniques. In [19], reflectometry is used with the objective of measuring the coil impedance. This coil is fed by a reflectometer's port by a coaxial line and its impedance is deduced from reflection coefficients measurement.

Other applicability of eddy currents is thickness measurement of a material. In [20] a pulsed eddy current system used to evaluate material thickness and properties is presented. An inductive and a giant magneto-resistive (GMR) sensor-based probe are used and then the results are presented and compared. Another example is [13], where a pulsed eddy current testing is also used to make the thickness of the specimen into uniform unit according to excitation frequency. Then it is used Fast

Fourier Transform (FFT) where is obtain the spectral component of the response signal and dividing the frequency regularly, the thickness is also divided into many units. For finishing, a variation of the frequency is obtained, and it is used to compute the thickness.

2.3. Structural Health Monitoring

The research on the field of SHM has been raising since 1970, however few industrial applications have resulted from this effort. SHM implements a damage detection strategy through the observation and monitoring of a structure continuously in order to identify the actual state of the structure. To accomplish that, the system must periodically measure structure’s characteristics and then analyze them. In SHM, function diagnosis may be considered as a new and improved way of making NDT, even though SHM is much more related to sensors integration, data transmission, computational power and processing ability inside the structures.

SHM has several advantages such as allowing a longer-lasting use of the structure, a reduced inactivity time, the early avoidance of catastrophic failures increasing safety, better cost efficiency, improvement of constructor’s products and changings on maintenance services. Structures with SHM have high reliability and low maintenance costs along with higher lifetime of the structure. The structures without SHM may see their reliability decreased as well as their lifetime and the maintenance costs end up increasing, as shown in Figure 2.12.

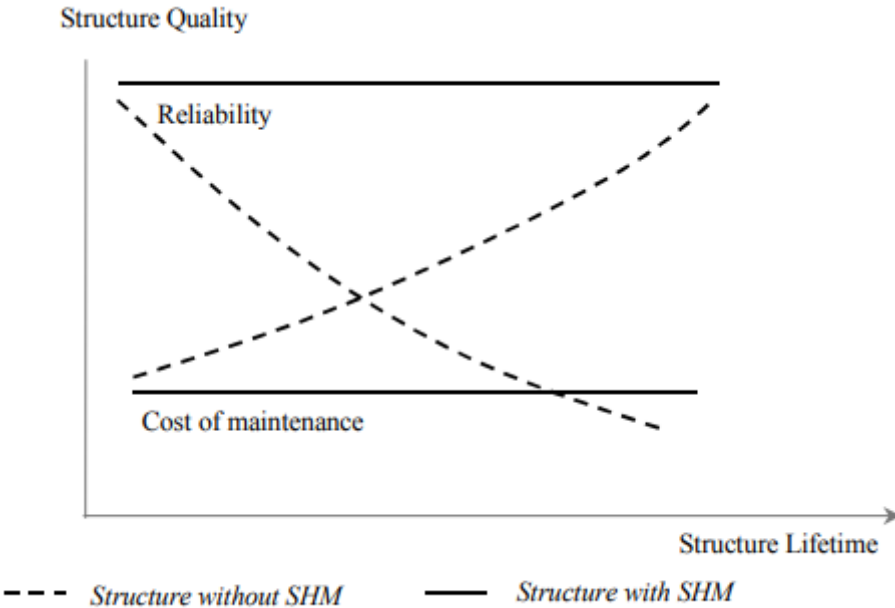



Figure 2.12 - Benefits of including SHM [21].

2.3.1. Structural Health Monitoring Categories

The range of areas which SHM operates is very wide and comprised by four categories: machine condition monitoring, global monitoring of large structures, large area monitoring and local monitoring. These categories are summarized in Table 2.1 [22].

Table 2.1 - SHM categories.

<i>SHM type</i>	Availability of standards	Type of Measurement	Applications in real systems	Number of sensors required
<i>Machine condition monitoring</i>	Many	Mainly passive	<ul style="list-style-type: none"> ➤ Multiple; ➤ Routinely applied in industry. 	
<i>Global monitoring of large structures</i>	Some	Mainly passive	<ul style="list-style-type: none"> ➤ Progressively more used but not mature; ➤ Many trials. 	
<i>Large area monitoring</i>	Limited	Mainly passive	<ul style="list-style-type: none"> ➤ Few commercial applications; ➤ Many trials. 	
<i>Local monitoring</i>	Limited	Mainly passive	<ul style="list-style-type: none"> ➤ Few specialist commercial applications; ➤ Many trials. 	

Machine condition monitoring is not exclusively related with structural health as it is considered a mature field that concerns about the condition of rotating machines. There are three maintenance strategies identified named run-to-break, time-based or usage-based preventive maintenance and condition-based maintenance. In [23], an analytical redundancy method is used which uses neural network modeling of the induction motor in vibration spectra to detect faults of a machine.

Global monitoring of large structures is also named Structural Identification, that is, establishing a numerical model of a dynamic system, based on its measured response, with major attention on evaluating the health and efficiency of the structure being monitored, and also making decisions about whether it needs maintenance or being replaced. The main application of this area is in large structures such as bridges. In [24], it is presented an acoustic emission (AE) and ultrasonic testing to monitor large concrete structures and it is showed the potential of AE to be a global monitoring technique, which aim is to examine large volumes with few sensors.

Large area monitoring category includes techniques which give full volume coverage of a segment in a large structure with the need of using a limited number of sensors. The aim of these techniques is seeking for localized damage even if, usually, there is a trade-off between the amount of area covered and sensitivity. The paper [25], introduces an omnidirectional guided wave inspection device, which comprises a circular array of electromagnetic acoustic transducer (EMAT) elements. This device enables the inspection of a large area of a metallic plate-like structure from a single location.

Local monitoring category of SHM incorporates methods that monitor only the area immediately next to the sensor, covering then a small area. The utility of local monitoring is to track the development of a damage previously identified with NDT inspection. The present work relates to a local monitoring technique. Another example of this category is [26], which uses a high-frequency vibration signature-based technique through a piezoelectric sensor on an aircraft structure.

2.3.2. Structural Health Monitoring Module

The SHM process usually relies on monitoring a structure over a certain period using suitable sensors to make some measurements and then analyze them to identify the current state of the structure. SHM systems involve a set of processes like measuring and collecting different parameters through sensors, analyze them and finally taking corrective actions.

As observable in Figure 2.13, the first part is composed by the function for monitoring the structure, which can be characterized by the kind of physical phenomenon associated with the damage monitored by the sensor, or by the kind of physical phenomenon used to produce a signal sent to the repository sub-system by the sensor. When having various sensors of the same type, they form a network and their data is blended with data from other types of sensors. To create a diagnostic, the controller uses the signal delivered by the integrity monitoring sub-system at the same time as the previous data is already registered. To finish, a similar structure management system connected to other structures can be considered a super system, allowing the health management of that super system.

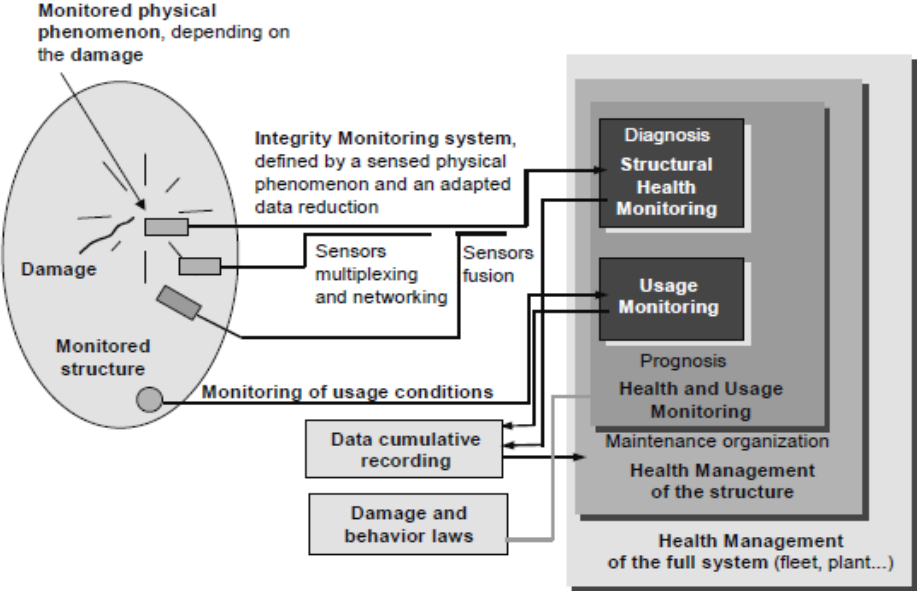


Figure 2.13 - Principle and organization of a SHM system [21].

2.3.3. Research and application

The implementation of SHM depends mainly on the use of sensors, and it can be applied to existing structures or to new ones. With this said, there are diverse techniques to implement SHM, such as using strain gauges sensors [27], fiber-optic sensors [28], piezoelectric sensors [29] [30], acoustic emission sensors [31], low frequency electromagnetic [32] [33], and capacitive sensors [34]. A comparison of some parameters between these techniques is present in Table 2.2. When the structure to monitor has a big area to covered, the fiber-optic sensors are a better choice than eddy currents sensors. However, if we need to monitor a small area with high sensitivity, inexpensive implementation and portable equipment, eddy currents sensors are the best to achieve the objectives.

Table 2.2 - SHM techniques comparison.

SHM Techniques	Acoustic Emission	Eddy currents	Fiber-optic	Piezoelectric	Strain Gauge
<i>Data analysis required</i>			X		X
<i>Embeddable</i>			X		X
<i>Expensive equipment</i>		X		X	X
<i>High data rates</i>	X		X	X	
<i>Inexpensive equipment</i>	X		X		
<i>Inexpensive to Implement</i>	X	X		X	
<i>Portable</i>	X	X		X	X
<i>Quick scan of large area</i>	X		X	X	
<i>Sensitive to small damage</i>		X		X	
<i>Surface mountable</i>	X	X			X

In [35], a SHM system is applied with vibrating wire strain gauges and the advanced fiber optic technology (such as distributed optical fiber strain sensing) to monitor the Qiantang River tunnel. This system is implemented due to the influence, in the normal service and structural safety, of the long-term impact in the tide of the Qiantang River.

Other application of SHM systems is the monitoring of bridges and [36] serves as an example of it. A support vector machine is applied and data from practical monitoring of Hangzhou Bay Bridge as the study object.

2.4. Internet of Things

IoT is a huge system created by blending network facilities and internet. In this way all components are connected with the network originating a system that can automatically identify, locate and monitor that component in real time.

2.4.1. Internet of Things organization

The core organization of IoT systems is based in four layers: perceptual layer, transport layer, treatment layer, and application layer. The perceptual layer corresponds to the physical layer and it is the base of IoT and its principal function is to percept, recognize and monitor/collect data from objects. The transport layer is equivalent to the traditional information transmission layer and its primary function is to allow information transmission between the perception layer and the treatment layer. The treatment layer implements intelligent processing of massive information through cloud computing, data mining and intelligent processing. Finally, the application layer is based in the other three layers and it is where

IoT completes the unification of information technology and different industries. In this case, the application layer is based in structural monitoring. All the layers described above can be observed in Figure 2.14.

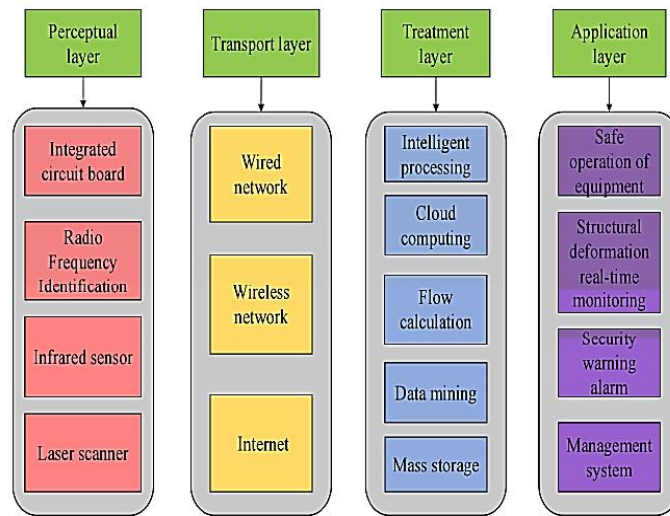


Figure 2.14 - IoT organization [37].

For the transport layer case, different wireless protocols are available and can be applied, as different applications require different wireless protocols. Table 2.3 presents six types of wireless protocols where three different characteristics of each can be observed: operation frequency band, maximum data rate and typical communication range. If a lot of information is generated and needs to be quickly transported to the treatment layer, one must opt for a Wi-Fi solution as its data rate is higher, but on the other hand if the ranges of communications are high the NB-IoT protocol should be the chosen. Inside of low-power wide area network (LPWAN) technologies are LoRa WAN, NB-IoT and SigFox. Lora is established for long-range and low-data-rate applications, NB-IoT has been regulated to be an integral part of the recently finished Third Generation Partnership Project (3GPP) Release 13 to address the requirements of IoT, and SigFox is used for IoT connectivity and is similar to cellular systems.

Table 2.3 - Wireless protocols.

<i>Protocol</i>	Operation Frequency Band (MHz)	Maximum Data Rate (kbps)	Typical Communication Range (m)
<i>Bluetooth BR/EDR</i>	2400-2483.5	2100	10
<i>LoRa WAN</i>	Regional sub-GHz bands 433 / 780 / 868 / 915	50	2000 ~ 14000
<i>NB-IoT</i>	LTE In-band, Guard band or Standalone 900	200	~ 22000
<i>SigFox</i>	Regional sub-GHz bands 868 / 902	0.1	3000 ~ 17000
<i>Wi-Fi</i>	2400-2500; 5725-5875	54×10^3	30
<i>ZigBee</i>	400-470; 800-960; 2400-2500	250	100

2.4.2. Advantages and disadvantages

IoT introduces several advantages such as increasing the acquired information to make better decisions, providing a better tracking system from objects and data, saving time used on the gathering and processing information, and if the cost of tagging and monitoring equipment gets low, the cost of IoT will also become lower.

However, IoT is not perfect and has some disadvantages like the lack of compatibility for the tagging and monitoring devices or equipment, the complexity of these kind of systems is huge which increases the chances of failure, the difficulty of providing safety service, and the bandwidth is limited for some applications.

2.4.3. Research and application

This concept has innumerable applications such as the creation of smart cities, improvement of structural health and traffic congestion, in the environment to detect forest fires and earthquakes, and in water to identify possible chemical leakages in rivers and pollution levels. IoT is also used in metering, security, retail, logistics, industry, agriculture, animal farming, domestic and health.

One example of a study that purpose implementing IoT in a city to transform it in a smart city is [38]. An IoT architecture is proposed, and considered IoT enabling technologies and IoT services to preserve the culture and implement revitalization in small towns.

2.5. Related work

The present work aim is to design a SHM system using with ECT to monitor a metallic structure. There are some examples of already proposed related work, some of them are described in this section.

A SHM system to monitor fatigue cracks of a metal structure through ECT is proposed in [39]. The sensor used is capable of measuring the crack with the accuracy of 1 mm, and the average error compared with fracture analysis is 4.6%. Another example of SHM with ECT is [33], where is used an eddy current sensor to identify damage in a conductive structure and it can detect the damage in the form of both corrosion and a small hole. In paper [7], a new technology using eddy current sensors is described, which promises to extend the life of aging aircrafts, reduce cost of inspection in difficult-to-access location and influence the design of new aircraft through the use of lighter components. A real case about the application of ECT in SHM systems is a product developed by Sensima Inspection, a company from Switzerland created in 2009. In the product sheet [40], the mode of operation of SHM-EC sensor is described. It is a remote inspection solution which aim is to have facility in applying on the crack to monitor and provide information on the evolution of the important values of the damage, such as its length and depth. That is, after the crack being discovered by NDT inspection, it will be continually monitored through the observation of the damage and lifetime evaluation. In other hand, the sensor can be applied to provide reports about crack initiation in crack-free locations

which have been previously determined as susceptible to cracking through the comparison with similar components or structure simulation.

Associating a SHM system in an IoT platform increases the value of it comparing with a normal SHM system. These new systems allow real-time data collections, data processing, event-driven and real-time decision-making [41]. They also have: high efficiency due to the facility of installing wireless sensor; high flexibility due to the facility of updating, adding, removing and replacing nodes; low cost. These advantages make the new SHM system better in performance because they are able to analyze and correlate data from strategic points [42]. The paper [43], resumes the advantages of implementing SHM systems associated with IoT in terms of autonomy, sampling rate, data sync and communication protocols.

In [44], the authors proposed a wireless sensor network for structural health monitoring with the vibration method to monitor civil structures. The sensor node is composed by accelerometers and is linked with a microcontroller that elaborate the data. Other example of this application is [45] which uses a wireless sensor network combined with different types of sensor technology, embedded computing technology and wireless communication technologies to evaluate the health of bridges. The sensors used to monitor the structure are ultrasonic and accelerometer.

On a different approach, to combine a wireless SHM system with ECT, the authors of [46] employed an eddy current based smart sensing system for online defect detection and identification in high speed drawn wires. The signal produced by the probe is fed to the signal processor unit that will processes the signal. This signal is acquired and displayed to the PC unit through the DAQ unit. The speed, simplicity, low cost, non-contact and non-invasive technique could make this a system that detects defect in real-time for large scale implementation.

Chapter 3 - Hardware

The final system focuses on monitoring the growth of a previously detected crack on a metallic material of a structure in an autonomous and permanent way. The system architecture is presented in Figure 3.1, where its different modules are represented.

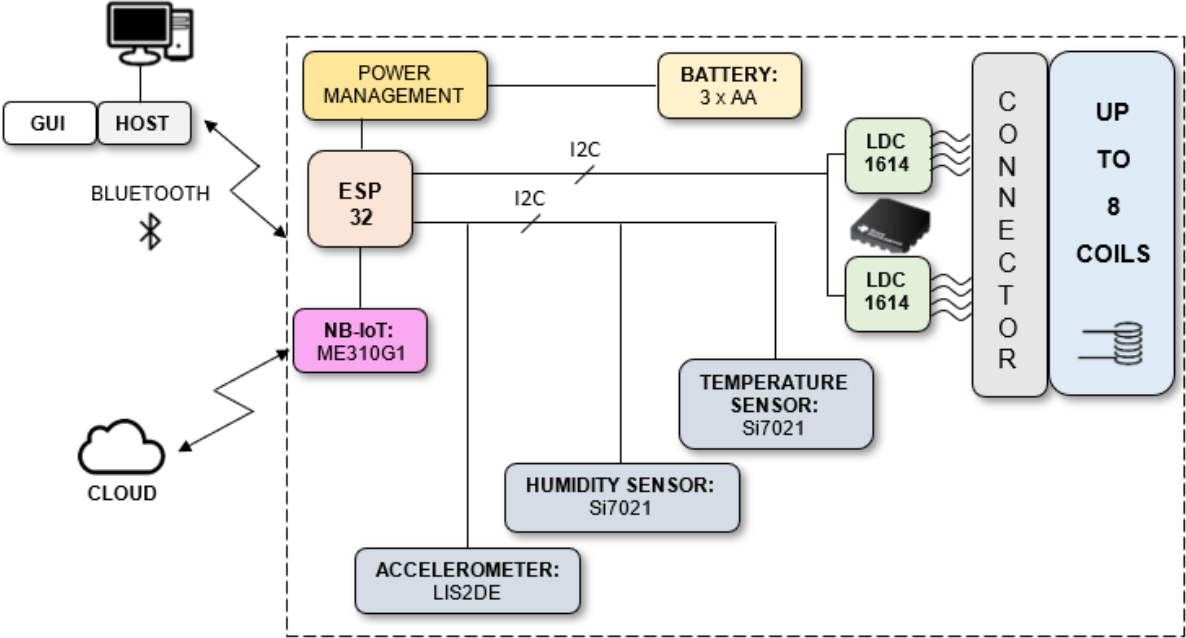


Figure 3.1 - System architecture.

The system is divided into five modules, each having its own function. The processor module is the one that controls all the devices and process the information gathered by the others four modules, therefore is the most important and indispensable one. The power management module ensures the operability of the entire system. The environment sensors are responsible for measuring external factors that may provoke changes in the test material. The ECT module receives and converts data collected by eddy currents' sensors into digital. The NB-IoT module enables the report of triggered alarms to the "cloud" environment. The hardware organization of the system follows the same division previously mentioned.

3.1. Processor

To process all the data collected from the sensors a microcontroller is needed, being Espressif Systems ESP32 the chosen one. The benefits of using the ESP32 chip microcontroller rely on its robustness to face the adversity of surroundings, performing in low-power mode, and also for having four more power modes, which is useful when the full usage isn't need. It also has an optimal trade-off between communication range, data rate and power consumption, being considered a highly-integrated solution for Wi-Fi-and-Bluetooth IoT applications. All these features make ESP32 perfectly suited to be included in the system. The functional block diagram of ESP32 is presented in Figure 3.2.

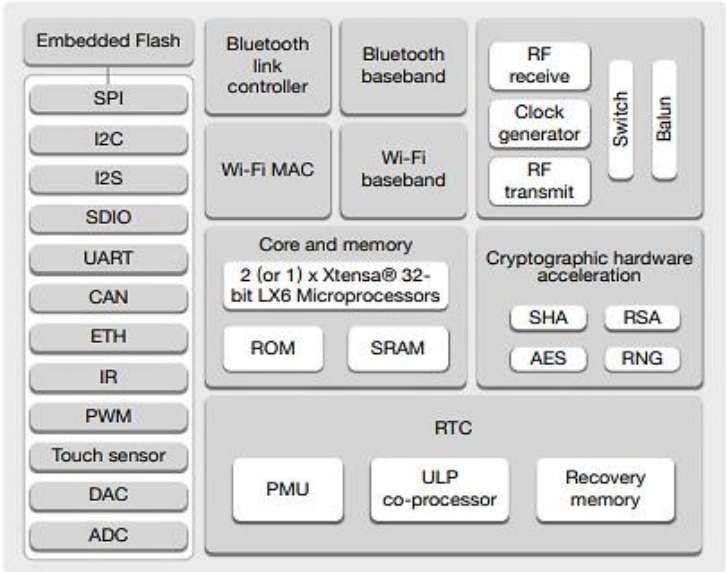


Figure 3.2 - Functional block diagram of ESP32 [47].

To expedite the prototyping process, an ESP32 Evaluation Board with a plugged in ESP32 microcontroller was used, through the section represented by letter C in Figure 3.3. This is a multi-purpose board, that offers low cost, high flexibility and availability. As identified in the same figure, the evaluation board is composed by a set of peripherals such as a header (A), buttons (B) and connectors (D), which allow an easy connection between ESP32, other integrated circuits (ICs) and the evaluation board.

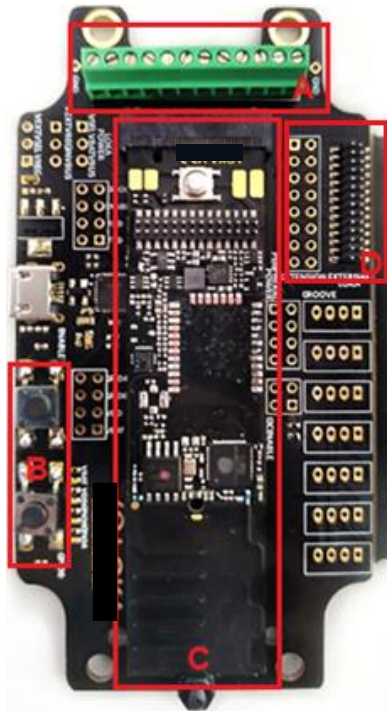


Figure 3.3 - ESP32 Evaluation Board.

ESP32 has forty-nine pins being eight of them, which are worth of mentioning with more detail, divided into two categories. Starting with the ESP32's digital pins, they are divided into three distinct power domains: VDD3P3_RTC, VDD3P3_CPU and VDD_SDIO. VDD3P3_RTC acts as input power supply for real-time clock (RTC) and central processing unit (CPU), VDD3P3_CPU is also the input power supply for CPU, and VDD_SDIO connects to the output of an internal low-dropout (LDO), whose input is VDD3P3_RTC. The internal LDO is automatically disabled when VDD_SDIO is linked to the same network as VDD3P3_RTC.

Other of the pin categories is the strapping pins. MTDI, GPIO0, GPIO2, MTDO and GPIO5 are the five strapping available pins. During ESP32's system reset, the latches of the previous pins sample the voltage level as strapping bits of '0' or '1', maintaining them until the chip is powered down or shut down. These bits are responsible for configuring the device's boot mode, the operating voltage of VDD_SDIO and some other initial system settings. The strapping pins are internally connected to pull-up or pull-down during the ESP32's reset. Therefore, when one of these pins is unconnected or connected to a high-impedance external circuit, the internal weak pull-up/pull-down is responsible of determining its default input level. The values of strapping bits are changeable through the application of external pull-up/pull-down resistances, or using the host microcontroller unit's (MCU) general purpose input/output (GPIOs), in order to control the voltage level of these pins while powered in ESP32. For this reason, the user needs to be very careful while connecting these pins to output ports of other ICs, as, during resets, the active values in these ports can modify the strapping options.

As said before, ESP32 processor integrates a Bluetooth link controller and Bluetooth baseband, which can carry baseband protocols and some other low-level link routines. Some of the features that the ESP32 Bluetooth radio and baseband support consist on high performance in Near Zero Intermediate Frequency (NZIF) receiver sensitivity with over 97 dB of dynamic range, power

management for low-power applications and, through the internal Static Random Access Memory (SRAM), allows full-speed data-transfer, mixed voice and data. The Bluetooth link controller operates in three major states denominated standby, connection and sniff. It permits several connections and other operations like inquiry and secure sample-pairing.

The chosen ESP32 version is the ESP32-D2WD with 4 Mbytes FLASH size. The processor is clocked at 26 MHz through a crystal oscillator, and connecting its outputs to the XTAL_N and XTAL_P pins of the chip. The antenna serving the wireless connection between the host was adapted from the module ESP-WROOM.

3.2. Power management

This is an essential module for the proper functioning of this system and its detailed representation can be observed in Figure 3.4. To power it, buck-only converters are the chosen due to their better pricing, availability and conversion efficiency. A buck converter consists on a switched DC-DC power converter that steps down voltage from its input to its output. The Diodes Incorporated AP3428 (U4 in Figure 3.4) is a switching regulator and allows a maximum of 5.5V power supply, setting the output to approximately 2.6 V. An important note is that this power supply is active while the main processor is “awake”, and it is efficient when the output current is high.

When the main processor is “asleep”, the fallback power supply is ensured by the Diodes Incorporated AP2138N-2.5 (U5 in Figure 3.4) LDO voltage regulator, whose output is fixed to 2.5 V. A LDO regulator is a DC linear voltage regulator which is able to regulate the output even if the supply voltage is really close to the output voltage. This has a better consumption rate when the output current is lower. To avoid leakage through the LDO pass device, the LDO output voltage must be lower than the buck converter output voltage.

To avoid leakage of the current through the buck converter, an additional circuit is required - the transistor (Q1) and respective gate control circuit. This transistor enters cutoff preventing current to flow through the DCDC output and feedback branches, when the buck converter enables signal DCDC_EN is de-asserted.

A set of three batteries of AA size with 1.5V each totalizing 4.5V was chosen due to the need of low power, portable and small source to power the device.

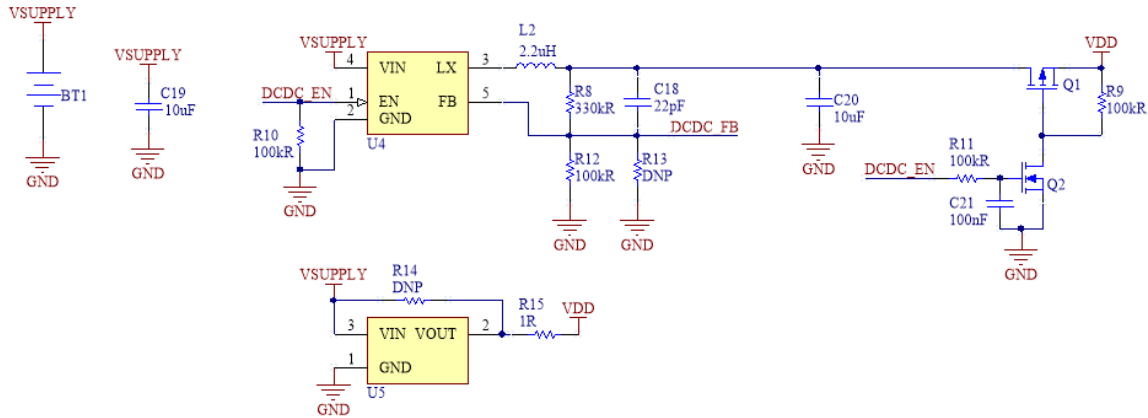


Figure 3.4 – Power management circuit.

3.3. Environment sensors

To analyze the surrounding environment where the structure to monitor is placed, three indicators were selected: temperature, humidity and acceleration.

To collect the temperature and relative humidity of the environment where the system is placed, the sensor of Silicon Labs Si7021 was used. The Si7021 provides low-power, high-accuracy, calibrated and stable solution, ideal to apply to an ample range of temperature, humidity, and dew-point applications.

It also integrates humidity and temperature sensor elements with an analog to digital converter (ADC), signal processing, data calibration, polynomial non-linearity correction and an Inter-Integrated Circuit (I²C) interface. The calibration data, from its individually factory-calibration from temperature and humidity, is stored in on-chip non-volatile memory. This feature guarantees a full interchangeability with no need to recalibrate or change. The functional block diagram of Si7021 is presented in Figure 3.5.

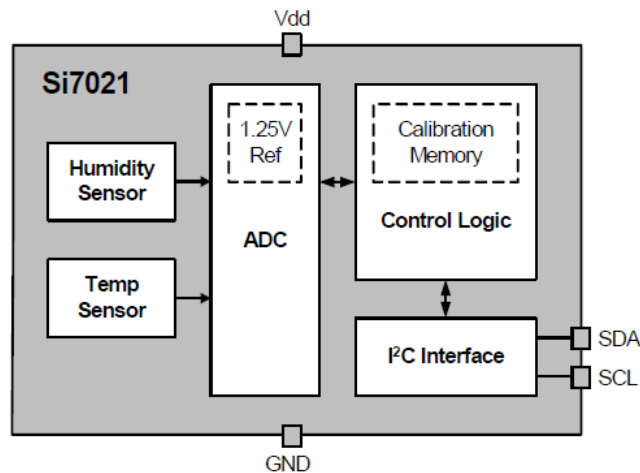


Figure 3.5 – Functional block diagram [48].

The low power consumption of this sensor is an important feature to this application, since its main function is not always required, and the device is meant to be battery powered. Si7021 has a wide operating range both of relative humidity and temperature. The relative humidity operating range is from 0 to 100 % and the temperature operating range is from -10 to 85 °C, with a ± 0.4 °C of accuracy.

Other indicator to be analyzed is the acceleration or the vibration that the system is being subject to. In order to acquire acceleration data, the ST Microelectronics LIS2DE12 accelerometer is used. This sensor can also collect temperature information, even though it is only used to measure acceleration. Figure 3.6 presents the block diagram that represents the acceleration measurement process. The entire measurement chain converts the capacitive unbalance of the Micro Electro-Mechanical Systems (MEMS) sensor into an analog voltage through a low-noise capacitive amplifier. The process is completed with the transmission of data through an I²C interface, after connecting the chip select (CS) pin to the voltage supply.

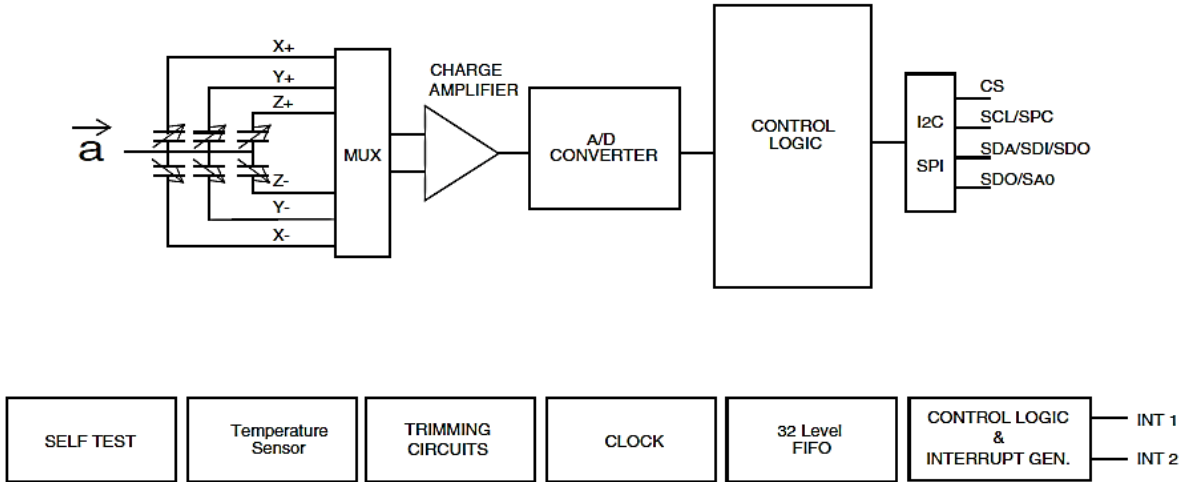


Figure 3.6 – Block diagram [49].

Like the previous sensor, LIS12DE12 is a low power sensor chosen for the abovementioned reason. Beyond this, the sensor is a nano 3-axis linear accelerometer. It has multiple full scales to available for selection $\pm 2g / \pm 4g / \pm 8g / \pm 16g$ and can measure accelerations with output data rates ranging from 1 Hz to 5 Hz. In this application we chose $\pm 2g$ full scale and 400 Hz data rate. In a normal application scenario, the device will work coupled to a static installation. Nevertheless, in our case scenario, the static acceleration will have a maximum of 1g on the possible axis, being this the reason why the $\pm 2g$ full scale fits our purpose. The dynamic acceleration, added to static one, will be low as the installation has no movement. This scale allows the best possible resolution with the 8-bits of the application ADC.

The LIS2DE12 sensor embeds a 10-bit wide, 32-level FIFO. FIFO, Stream, Stream-to-FIFO and FIFO bypass are the four operation modes allowed due to buffered outputs. If FIFO bypass mode is activated, FIFO remains empty and do not operate. However, if the FIFO mode is activated, measurement data from acceleration sensorial detection on the x, y, and z-axes are stored in the FIFO buffer.

3.4. Eddy Current Testing

The ECT module includes two sets of four-channel Inductance-to-Digital Converters (LDC), so the device can read up to eight coils. Texas Instruments LDC1614 was the chosen, which converts the

inductance collected through sensors to a digital value for later analysis by the processor. The LDC1614 also communicates through an I²C interface.

The function of LDC1614 is to measure the oscillation frequency of multiple LC resonators. The output of the device is a digital value proportional to frequency, with a measurement resolution of 28 bits. The frequency measured can be converted to an equivalent inductance, or, instead, depending on the application, mapped to the movement of a conductive piece. The LDC1614 can support a wide inductance range and capacitor combinations with oscillation frequencies varying from 1 kHz to 10 MHz, containing equivalent parallel resistances as low as 1.0 kΩ. The simplified schematic of LDC is present in Figure 3.7.

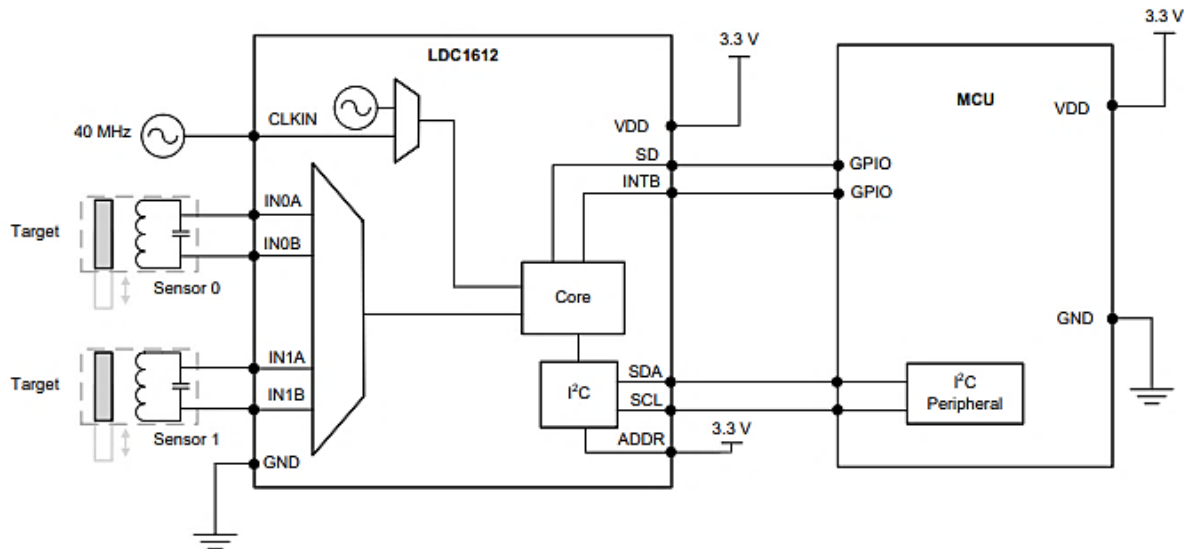


Figure 3.7 – Simplified integration of the LDC1612 with an MCU [50].

The functional principle relies on having conductive objects in contact with an alternating current (AC) electromagnetic (EM) field that consequently induces field modification, which can be detected through a sensor. An inductor along with a capacitor build an L-C resonator, also named L-C tank, capable of producing an EM field. With a L-C tank, the effect caused by a disturbance is the apparent shift in sensor's inductance, that can be seen as a shift in the resonant frequency. The LDC measures the oscillation frequency of the L-C resonator. In more detail, it has front-end resonant circuit drivers, followed by a multiplexer that selects through the active channels, connecting them to the core that makes the measurements and digitalizes the sensor frequency. To measure it, the core uses a reference frequency (f_{REF}) which derives from either the internal reference clock (oscillator), or an externally supplied clock. To support device configuration and to transmit the digitized frequency values to the host processor LDC1614 uses an I²C interface. The block diagram of LDC1614 can be shown in detail in Figure 3.8.

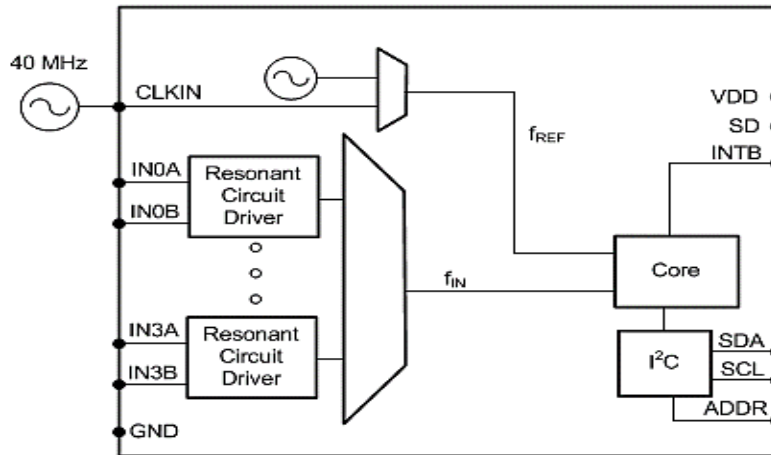


Figure 3.8 – Detailed block diagram of LDC1614 [50].

The reasons why LDC1614 is the chosen converter rely on having multiple high-resolution channels supporting remote sensing, performing with low cost, power and size, and being a compact solution with a decreased number of needed ICs. These features make this converter very useful for SHM applications.

Other of LDC1614's important advantages which were beneficial to this work were the precision dependence on the resonant driver circuit, the chosen capacitor and oscillator. This last one stands as the most critical, so we use external temperature compensated oscillators for better accuracy.

To test the LDC1614 front-end, LDC1614 Evaluation Module (LDC1614EVM) is used for inductance to digital conversion through sample PCB coils. This module provides maximum evaluation and system design flexibility, includes example sensor coils, operates via PC, it is supported by a Graphical User Interface (GUI), uses LDC1614EVM which has the major advantage of accelerating the prototyping of the end application.

3.5. Narrowband-IoT

The NB-IoT module consists on the Telit ME310G1 and is used to prepare the hardware of the device for alarm reporting to the cloud. It allows the implementation of low-cost IoT component that is small in size and has a low power consumption. ME310G1 is compliant to 3GPP Release 14 Cat M1/NB2, that enables increased power saving for IoT applications, through the use of Power Saving Mode (PSM) and extended Discontinuous Reception (eDRX). This allows devices to wake up periodically while delivering only the smallest quantity of data needed before returning to sleep mode. The improved coverage supports superior in-building penetration when compared to previous cellular Long-Term Evolution (LTE) standards. The devices with LTE Cat M1/NB2 are developed with small cost, size and power consumption. 3GPP Release 14 adds techniques to increase the data transfer rate for LTE-M and NB-IoT.

ME310 has LTE user equipment (UE) category M1 (1.4 MHz) / NB2(200 KHz), a single antenna, SIM application Tool Kit 3GPP TS 51.01, and IPv4/IPv6 with TCP and UDP protocol. The chip has a 94-pad Land Grid Array (LGA).

3.6. Printed Circuit Board

To achieve the goal of the project, a Printed Circuit Board (PCB) was designed. It is a 2-layer PCB board, with 50 x 100 mm, that includes the remaining module for fulfilling the proposed system.

The modules previously described are divided into sections in the PCB shown in Figure 3.9. The antennas needed enable the Bluetooth (right) and the NB-IoT (left) are placed on the top of the board represented by the letter A. Going down, letter B contains the processor module with ESP32 and 26 MHz crystal oscillator. With the letter C is represented the footprint of the ME310G1 module, but not soldered because this module is not available until this date. Because of that, all components that support it are also not soldered. Letters E and D represent the power management module, being, by the same order, the switching regulator and the linear regulator. The peripherals zone is in the bottom part of the board. One of the two LDC1614 of the ECT module is placed in letter F, and, in spite of the existence of a board hardware ready to read up to eight coils, in this project just one was soldered. To connect the probes to the LDC a header, represented by letter H, was used. In letter G the environment sensors module with the Si7021 and the LIS2D12 sensors are visible. A battery holder was welded in the bottom layer of the PCB to avoid interfering with the other components placed in the top layer.

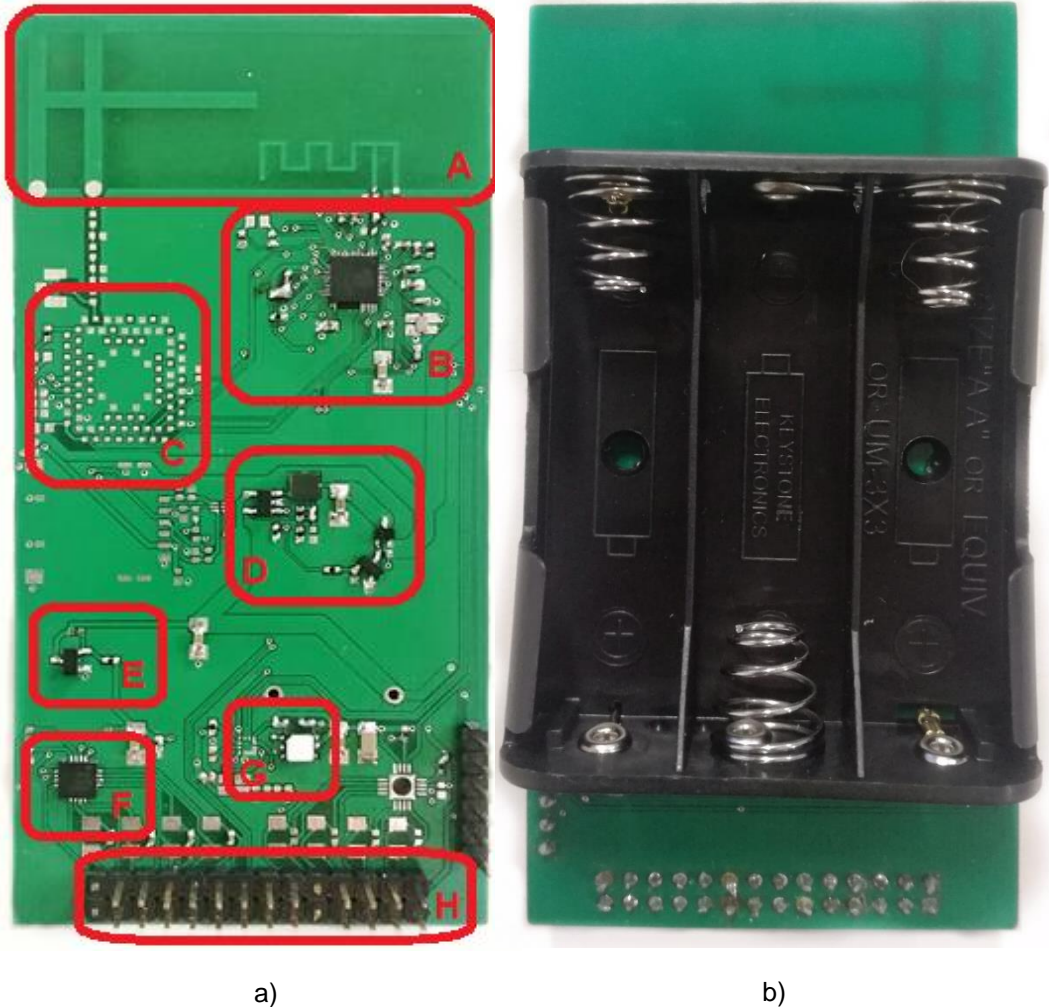


Figure 3.9 - Main Board PCB top layer (a) and bottom layer (b)

Chapter 4 - Firmware and Software

The objective of this project is to develop a device, able to implement the ECT method in a SHM procedure, which can be placed to monitor a structure in an autonomous and permanent way. The programming stage of the whole project is divided into the serial protocol chosen to communicate between the peripherals and the device, and the communication protocol that was developed to achieve the proposed objectives and the GUI responsible to control the communication and present all the results of measurements.

4.1. Communication protocol

The device communicates with the host is based on a communication protocol created in specific to this application to complete the purpose stated. This is a control protocol ready for any serialized data communication interface. In this case, a host computer, an electronic instrument, and at the board level with a master micro-controller and its dedicated peripheral are needed.

4.1.1. Protocol description

The protocol established allows bi-directional transmission of several elements is composed of commands and which command is divided into four variables of type unsigned integer in big-endian format. These variables are named function, value, size, and data. Table 4.1 resumes the characteristics of each field of a command.

Table 4.1 - Command description.

Command field	Length	Definition
<i>Function</i>	4	Defines the action or configuration to make or adjust
<i>Value</i>	4	Used when only a single parameter is required, and for example to identify a channel
<i>Size</i>	4	Zero if no more data is required or to specify how much additional bytes shall be received
<i>Data</i>	4 * Size	A variable size array with the remaining elements required to the function

To implement the command a data structure is defined through C++ language. In Figure 4.1, it can be analyzed, showing that the struct includes memory for the three header fields and a pointer for the array dynamically allocated memory.

```
typedef struct command_def {  
    int function;  
    int value;  
    unsigned int size;  
    unsigned char* data;  
}command_t;
```

Figure 4.1 - Command structure.

Knowing the previous command structure, the slave waits for the reception of the complete command header, that in this case are twelve bytes (four bytes for the function plus the value plus the size). It analyzes the size field and if the result is different from zero, the system receives an extra data with size equals to 4*size field on dynamically allocated memory. The slave application layer has the responsibility for interpreting the command struct and reply. The commands with the necessity of a reply, the slave unit has to reply with the respective data. In other way, an acknowledge command, with the same field function and value (equal to 1) will be replied.

In order to be able to manipulate and move the command_t structure, it is created three functions named build_command, receive_cmd, and send_cmd. The build_command function is a void-returning function and is the one that can form the command_t structure receiving as arguments a pointer to a command_t variable, an integer that establishes the function field, an integer representing the value field, an unsigned integer determining the size field and a pointer to an unsigned char variable data. To receive a command from the host, the void received_cmd function is created and has as argument a pointer to a command_t variable. This function accesses to the first twelve bits and one by one puts them in the command header, and if the size field is different from zero it puts the rest of the value in the data field. To send a command to the host side there is the void send_cmd function, which also has as argument a pointer to a command_t variable. It writes directly through a Bluetooth class function the first twelve bits, and then if the size item is different from zero send the data field.

4.1.2. Commands explanation

To complete the whole system, there are seventeen commands defined in the program and they are divided into two types: acknowledge commands and general commands. Acknowledge commands are the ones used to confirm the reception and execution when no specific data is required to be transmitted from the device to the host. General commands, that are the majority, which allow the device configuration and trigger the readout of the diverse sensors' interfaces.

The acknowledge commands include the OK acknowledge, as the name implies, is an OK message reporting that the whole occurs with no errors, and the NOK acknowledge which is a message informing that the transmission was not correctly completed. In Table 4.2 there are two examples of commands definition, one with the size equal zero and other with size field different than zero. The read humidity command has a required sized of zero because it does not need more data to perform its action. In contrast, the change frontend conversion time function needs one more argument, it means a

size value of four because one integer has four bytes size. The complete list of commands is filed in Appendix I.

Table 4.2 - Commands definition example.

<i>Command name</i>	<i>Function</i>	<i>Value</i>	<i>Size</i>	<i>Data</i>	<i>Direction</i>
<i>Read humidity</i>	0x21	1	0	NULL	Host to Device
<i>Change frontend conversion time</i>	0x65	Channel	4	RCOUNT	Host to Device

4.2. Peripherals readout

As specified in the Hardware section, all the sensors communicate with the processor through an I²C interface. The peripherals to be read are divided into two parts. There are environment commands where the read temperature, read humidity and read acceleration functions are called, and the LDC1614 commands where all the functions reserved to this peripheral are called.

4.2.1. I²C interface

I²C is a serial protocol where a single master can control multiple slaves or multiple masters can control both single or multiple slaves, one possible representation is Figure 4.2. It uses only two wires to complete the interface, the serial clock (SCL) is the line that carries the clock signal and the serial data (SDA) is the line where master and slave send and receive data.

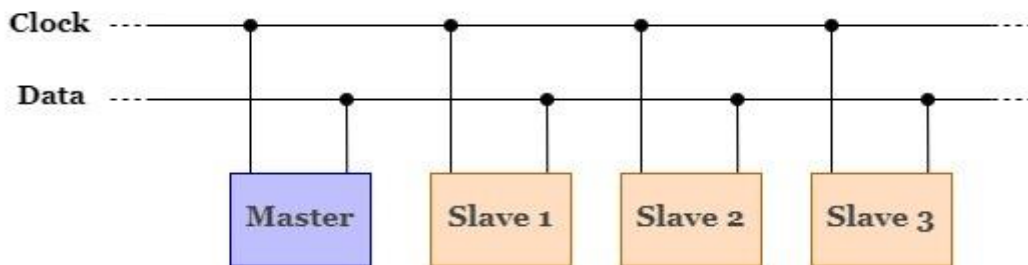


Figure 4.2 - I²C Interface buses.

To start the transmission of data the master sends a START condition, which is defined as a HIGH to LOW transition on the SDA line, while the SCL line is held HIGH. When this happens, the bus goes into a busy state. To identify which slave does the master wants to connect, it sends the 7-bit base slave address. To complete the 8-bit address, the master needs to send the WRITE bit (0). After the slave identification and the message is successfully received, the slave sends back to the master an acknowledge (ACK) bit (0). Then the master sends a byte with the command that it wants to slave preform. The salve needs to send an acknowledge bit to finish the first part of the sequence to perform a measurement. The second part starts with a START signal sent by the master, that is a change to LOW on the SDA line while SCL remains HIGH. It is also sent again the 7-bit base slave address but

this time a READ bit (1) is sent because the action to perform is read the measurement made. If the address is successfully transmitted, an ACK bit from the slave is sent and then a byte of data is transmitted. If the master is only receiving one byte of data from the slave, it sends a no master acknowledge (NACK) and, right away, sends a STOP condition. A STOP condition is a LOW to HIGH transition on the SDA line, while the SCL line is held HIGH.

4.2.2. Temperature and Humidity sensor

After the read temperature and read humidity functions are invoked, temperature and humidity are collected through the Si7021 sensor that communicates with the processor module through an I²C interface, as mentioned before. The 7-bit base slave address of the sensor is 0x40.

This sensor allows two methods to indicate to the master that the measurement is in progress. The hold master mode where clock stretching is verified and the no hold master mode where a NACK is requested after the 7-bit slave address with the READ bit is sent. In spite of the hold master mode is the method that takes more time to perform the measurement, it is the one that is more reliable, and for that reason, the method used is hold master mode. As soon as a relative humidity measurement has been made, the data resulted from this measurement need to be converted to percent relative humidity. This conversion can be made by

$$\%RH = \frac{125 * RH_Code}{65536} - 6, \tag{4.1}$$

where %RH is the measured relative humidity value in percent relative humidity, RH_Code is the 16-bit word returned by the Si7021. Every time a relative humidity measurement is made, it is necessary to do a temperature measurement because of temperature compensation of the relative humidity measurement. However, if the temperature value is needed, there is a specific command that returns the temperature value measured at the time relative humidity is measured. The data returned from the sensor may be converted into degrees Celsius (°C) through

$$Temperature(^{\circ}C) = \frac{175.72 * Temp_Code}{65536} - 46.85, \tag{4.2}$$

where Temperature(°C) is the measured temperature in °C, and Temp_Code is the 16-bit word returned by the Si7021. The commands that allow the identification of the action to be performed is in Table 4.3.

Table 4.3 - Command description of Si7021.

Command Description	Command Code	Type
<i>Measure Relative Humidity, Hold Master Mode</i>	0xE5	Read
<i>Measure Temperature, Hold Master Mode</i>	0xE3	Read

4.2.3. Acceleration sensor

When calling the read acceleration function the acceleration of the device is collected by the LIS2DE12 sensor through an I²C interface. The 6-bit base slave address is 001100xb, the least significant bit (LSb) is modified with SA0 pad. If the SA0 pad is connected to the voltage supply, LSb is '1', in another way if the SA0 pad is connected to ground, LSb is '0'. In this hardware the SA0 pad is connected to ground, therefore the 7-bit base slave address of the LIS2DE12 is 0x18.

To communicate with the sensor the master device needs to use several defined commands, present in Table 4.4. To launch the accelerometer sensor, it starts with the initialization of the I²C interface and then read the WHO_AM_I register. If the register returns 0x33, the data rate is set to 400 Hz, the three-axis reading is enabled, the full-scale is set to $\pm 2g$, the interrupts in INT1 and INT2 pin are disabled and sets the FIFO to bypass mode. After this, the accelerometer collects the acceleration of each axis. The data acquired is then divided by 63 that is the divider associated with $\pm 2g$ range.

Table 4.4 - Commands description of LIS2DE12.

<i>Command Description</i>	<i>Command Code</i>	<i>Type</i>
<i>Read WHO_AM_I register</i>	0x0F	Read
<i>Disable interrupts on the INT1 pin</i>	0x22	Read/Write
<i>Disable interrupts on the INT2 pin</i>	0x26	Read/Write
<i>Select the bypass FIFO mode</i>	0x2E	Read/Write
<i>Setting data rate and enable axis</i>	0x20	Read/Write
<i>Setting the full-scale</i>	0x23	Read/Write
<i>X-axis acceleration data</i>	0x29	Read
<i>Y-axis acceleration data</i>	0x2B	Read
<i>Z-axis acceleration data</i>	0x2D	Read

4.2.4. Inductance-Digital Converter

The final peripheral is the LDC1614 that needs to be configured and its channels connected have to be read. To configure the LDC there are seven parameters to define, to do this the processor communicates with the converter through an I²C interface. The LDC1614 can have two 7-bit base addresses depending on whether the ADDR pin is connected to ground or the same pin is connected to the voltage supply. If the ADDR pin is set low the 7-bit base address is 0x2A, however, if the ADDR pin is set high the 7-bit base address is 0x2B.

Beginning with which reference clock it is used, it can be an internal clock or an external clock. The internal clock is an internal limited accuracy oscillator with a typical frequency of 43 MHz, the

external clock can be supplied by an external oscillator when better accuracy is required. To accomplish it, the device needs to change the *REF_CLK_SRC* bit of the LDC1614 *CONFIG* register and when completing the configuration of this parameter, the device must confirm the success of it.

Then, the LDC1614 has four input deglitch filter bandwidths (1 MHz, 3.3 MHz, 10 MHz, 33 MHz) and it is recommended to select the lowest setting that exceeds the highest sensor oscillation frequency. To achieve it, the device has to change the *DEGLITCH* bit of the LDC1614 *MUX_CONFIG* register and after completing it, the device has to validate the success of this.

Another specification to be set is the conversion time that can be done by programming the reference count. It is possible to determine the conversion time register value by

$$RCOUNT_x = \frac{t_{CX} \times f_{REFx}}{16}, \quad (4.3)$$

where *RCOUNT_x* is the conversion time register value of channel *X*, *t_{CX}* is the conversion time for any channel *X*, *f_{REFx}* is the reference frequency of channel *X*. In general, a longer conversion time provides a higher resolution inductance measurement, being 0xFFFF required for full resolution. To accomplish it, the device has to change the LDC1614 *RCOUNT_x* register and when the configuration of this parameter is complete, the device needs to confirm that this was accomplished.

One more step is changing the conversion offset value, which is a value that may be subtracted from each DATA value to compensate for a frequency offset or maximize the dynamic range of the sample data. The conversion offset value can be obtained from

$$OFFSET_x = \frac{f_{OFFSETx}}{f_{REFx}} \times 2^{16}, \quad (4.4)$$

where the *OFFSET_x* is the offset value set in the *OFFSET_x* register, *f_{OFFSETx}* is the frequency offset register and *f_{REFx}* is the reference frequency of channel *x*. In this way, the device has to change the LDC1614 *OFFSET_x* register and when completing the configuration of this parameter, the device has to confirm the success of it.

Then, the sensor activation time is the amount of settling time needed for the sensor oscillation amplitude to stabilize, and the settling wait time is programmable. To complete this configuration, the device has to change the LDC1614 *SETTLECOUNT_x* register and when finishing it, the device must validate it.

There is also a need to change the channels reference clock divider, which has the *FIN_DIVIDER_x* and the *FRER_DIVIDER_x*. To achieve it, the device needs to change the previous fields in LDC1614 *CLOCK_DIVIDER_x* register and when completing the configuration of this parameter, the device answers the validation of the action.

Other parameter to take in count is the drive current, and the *DRIVE_CURRENT_x* register is composed of *IDRIVE_x* and *INIT_DRIVE_x* fields. The first field is the drive current used during the settling time and conversion time for channel *x* and the second one is the initial drive current stored during autocalibration. To perform the configuration, the device has to change the LDC1614 *DRIVE_CURRENT_x* and after completing the configuration of this parameter, the device has to confirm the success of it.

To finish the LDC1614 configuration there is an important command that is capable of resetting the device. To achieve it, the device needs to write in LDC1614 *RESET_DEV* register that stops any active conversion and all registers return to their default values and, then, to confirm the success of this action.

When the LDC1614 configuration is done, the next step is the collection of data of the several probes connected to the LDC1614. To do this there are two methods of present the result of measurements. It can only show the outcome of one acquisition per channel or the continuous acquisition per channel as the previous method. To accomplish the acquisition, the device needs to read the *DATA_MSB* register and the *DATA_LSB* register in this same order. After the collection of data been completed, the device must send the measurement result to the host. The data received has to suffer one conversion from digital to the inductance International System of Unit (SI) that is the henry (H). to do this, first, it needs to calculate the frequency sensor by

$$f_{sensor} = \frac{DATAx \times f_{REFx}}{2^{28}}, \quad (4.5)$$

where f_{sensor} is the sensor frequency, $DATAx$ is the digitalized sensor measurement for each channel and f_{REFx} is the reference frequency for each sensor. After calculating f_{sensor} through (4.5), it has to calculate the inductance through

$$f_{sensor} = \frac{1}{2\pi\sqrt{LC}}, \quad (4.6)$$

where f_{sensor} is the sensor frequency as previously denominated, L is the inductance in henry and C is the capacitor in parallel with the probe coil the probes in Farad. To present the measurement of the continuous acquisition, the host has a graphical application with a graphic per channel. The commands that configure and allow the readout of the channels connected with LDC1614 are in Table 4.5.

Table 4.5 - Commands description of LDC1614.

Command Description	Command Code				Type
	CH0	CH1	CH2	CH3	
<i>Conversion Configuration</i>	0x1A				Read/Write
<i>Channel Multiplexing Configuration</i>	0x1B				Read/Write
<i>Reference Count setting</i>	0x08	0x09	0x0A	0x0B	Read/Write
<i>Offset value</i>	0x0C	0x0D	0x0E	0x0F	Read/Write
<i>Settling Reference Count</i>	0x10	0x11	0x12	0x13	Read/Write
<i>Reference and Sensor Divider settings</i>	0x14	0x15	0x16	0x17	Read/Write
<i>Current drive configuration</i>	0x1E	0x1F	0x20	0x21	Read/Write
<i>Reset Device</i>	0x1C				Read/Write
<i>MSB Conversion Result and Error Status</i>	0x00	0x02	0x04	0x06	Read
<i>LSB Conversion Result</i>	0x01	0x03	0x05	0x07	Read

The LDC1614 driver includes also the possibility of the device working in an autonomous mode, constituted by the store, load and automation functions. Starting with the store command, it stores the current configuration, defined by the host, permanently for later use on autonomous mode. For this, the device has a `ldc_conf` structure array with four positions, representing the four channels, which field is defined as shown in Figure 4.3. The structure is saved in non-volatile memory using the function `nvs_set_blob`. For the host to have access to the previously stored configuration, it has the load function that is able to read the `ldc_conf` structure variable, through the `nvs_get_blob` function, and to send it back to the host. To complete the automation, the automation function is called, and with the access to the `ldc_conf` structure variable stored previously, perform the configuration of LDC1614 and the readout of the active channels. This function after configuring the LDC1614 active channels performs the readout of the channel for 10 seconds. The readout of the active channels is represented in four graphic items in the interface. When there is a significant change in the readout value compared to the last value read, there is an alert message that appears in the interface indicating a fault identification. The significant change value is defined in a threshold value saved on the host side.

```
typedef struct ldc_conf_def {
    uint32_t active;
    uint32_t ref_clock;
    uint32_t deglitch;
    uint32_t rcount;
    uint32_t offset;
    uint32_t settlecount;
    uint32_t clock_divider;
    uint32_t drive_current;
}ldc_conf;
```

Figure 4.3 - LDC1614 configuration structure,

4.3. Code organization

To program the device with all commands previously named, it is used a Virtual Machine (VM) with Eclipse, an integrated development environment (IDE), in the C++ language. To organize all the programs, it was divided into nine folders categorized by the main application focus. Which folder has a `.cpp` file, where the real action of which function is coded, and a `.h` file, that is the header file.

The folders reserved for communication are the `ESP32_Bluetooth` folder, the `I2C` folder, and the `Serial_Protocol` folder. The first one is where the functions reserved to the Bluetooth are programmed, like initializing and disabling the Bluetooth module, starts the Serial Port Profile (SPP), and verify if there is a connection concluded. The `I2C` folder is where there are the functions that can initialize `I2C` interface in master mode, and allow reading and sending data through `I2C` communication between the ESP32 and the sensors. Finally, the `Serial_Protocol` folder is where the previous description of the `command_t` structure is defined and the functions `build_command`, `receive_cmd`, and `send_cmd` are defined.

To process the information gathered through the communication functions, there are the `LDC1614_Commands`, `Si7021` and `LIS2DE12` folders. The first one is where there is the definition of the several commands already explained that refer to LDC1614. The `Si7021` is the folder where the functions `si7021_init` (initialize `I2C` Si7021 sensor), `si7021_humidity` (acquire the humidity value) and

si7021_temperature (collect the temperature value) are defined. The LIS2DE12 folder has the functions lis2de12_setAxis, lis2de12_setRange and lis2de12_setDataRate called in the lis2de12_init function to initialize the I²C communication and the accelerometer LIS2DE12, and to collect the acceleration of which axis has the lis2de12_readAxis function.

To perform in autonomous mode, the program has the LDC_Config and the Automation folders. The first one is where the ldc_conf is defined, and the Automation folder is where the functions load, store, and automation are defined. All of these functions were previously explained.

To gather all the functions to be called there is the interface folder. This folder has the i2c_interface function where after receiving a command select through the command→function value which function it has to run.

The principal folder is where the main file is programmed. It starts with the initialization of the Bluetooth module, and then it waits two minutes until some Bluetooth host connects with the device. When it happens, the device waits for a command sent by the host and then it calls the interface function. If there is no host to connect with it jumps directly to the autonomous mode.

4.4. Graphical User Interface

As said in sub-section 4.3, a VM with Eclipse with C++ language is used to define the commands. However, there is a need to create an interface to allow users to control these commands. This same interface is developed in Spyder, an open-source multi-platform IDE written in Python, for Python applications, in this case, it is Python 2.7. Therefore, the language with which the GUI is programmed in Python with the TraitsUI library project and the toolkit used is PyQt4. PyQt4 is a set of Python binding for Digia's Qt multiplatform GUI toolkit.

Figure 4.4, Figure 4.5, Figure 4.6 and Figure 4.7 represents the four tabs that compose the GUI. The first tab, represented in Figure 4.4, that appears when running the program is the one reserved to connect or disconnect with a device through Bluetooth, to LDC1614 configuration and to read a single value from the probes.

The Commands definition tab has a Connect button (A) after being pushed the search for Bluetooth serial ports opened to connect and when a port is found the device is actually connected with the host. The Disconnect button (B) disables the Bluetooth module of the ESP32. To program the LDC1614 with the respective commands explained in 4.2.4 and defined in Appendix I the Program button (C) is pressed and to reset the LDC1614 configuration the Reset button (D) is the one. To collect a single value of one or more probes, it is needed to push the Read button (E). To choose which channels to program or read, it is required to enable the checkbox (F) below the title.

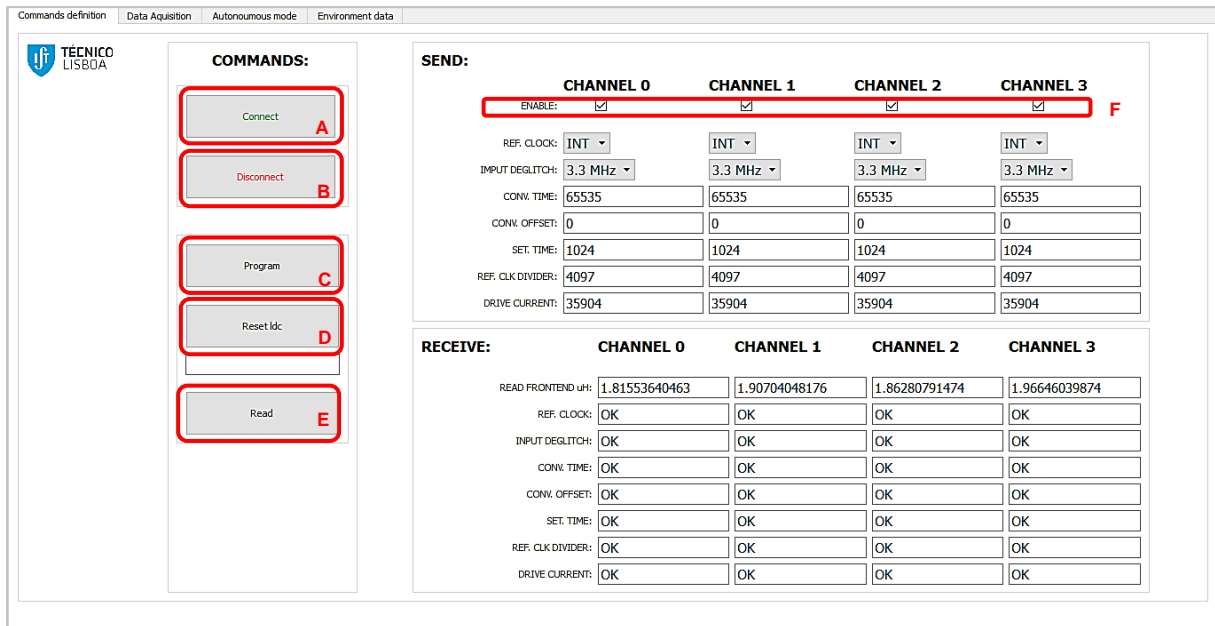


Figure 4.4 - Command definition tab.

The second tab, in Figure 4.5, presents the continuous reading of the four inductance sensors with the start and stop control buttons. In the Data Acquisition tab, there is a Start (A) and Stop (B) button. The Start button only can be pushed after choosing which probe or probes the user wants to collect continuous data from. To stop this collection the Stop button is pressed and the checkbox became enable.

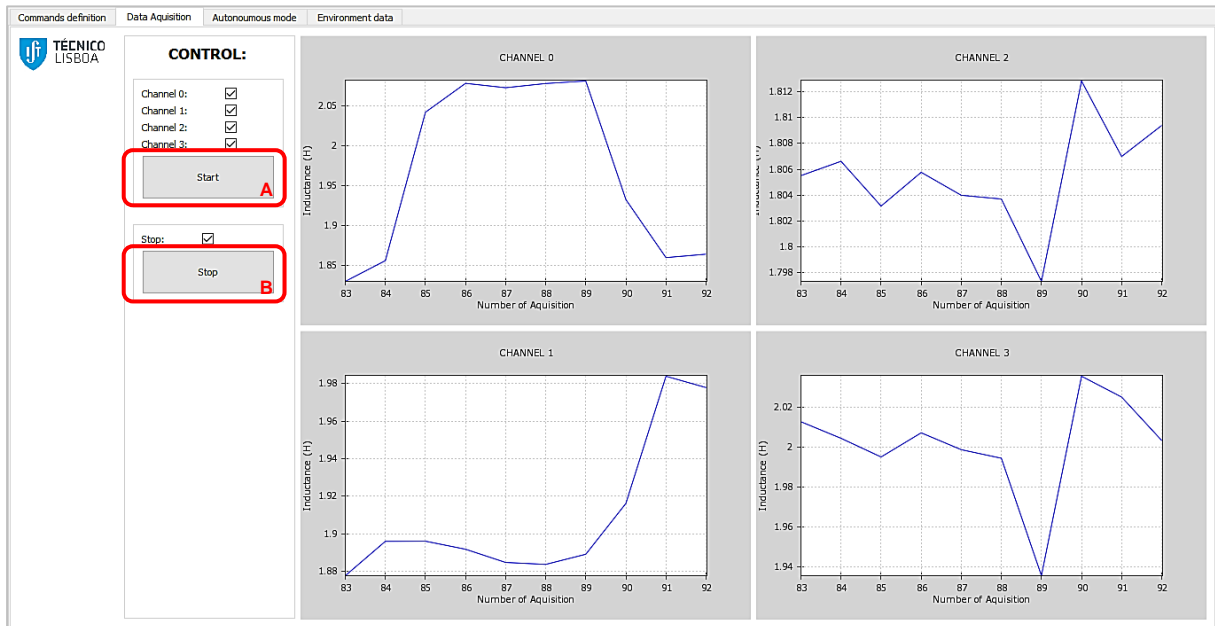


Figure 4.5 - Data acquisition tab.

The third tab, that is in Figure 4.6, is reserved to store the values presented in the first tab or to load to them the last values stored on the device, and to represent the values collected in the autonomous mode. The Autonomous mode tab has three buttons. The Load button (A) that calls the load function previously described, the Store button (B) that runs the store function also previously

explained and the Automation button (C) that program the LDC1614 with the last configuration stored and collects for 10 seconds data from the channels defined active in the last configuration stored.

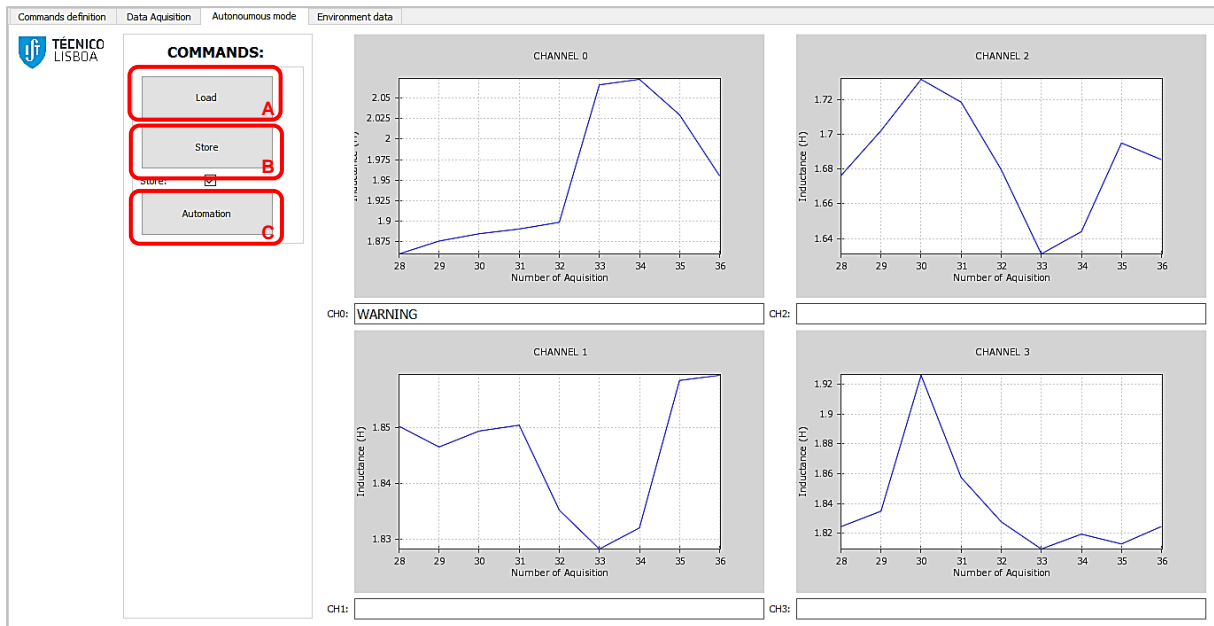


Figure 4.6 – Autonomous mode tab.

The fourth and final tab, presented in Figure 4.7, is where it is shown the environment sensors' results. The Environment data tab is the only one with one button. The Read environment button (A) requests the temperature, relative humidity and the acceleration of the three axes to device and presents the value in the spaces below.

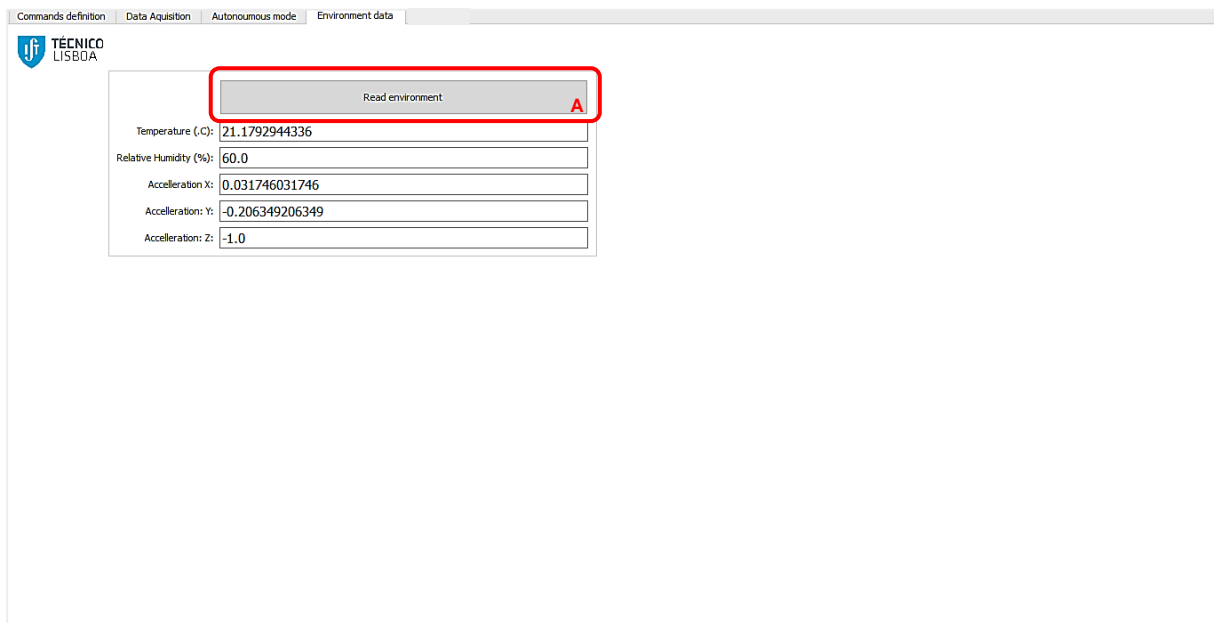


Figure 4.7 - Environment data tab.

4.5. Main execution flow

To resume the main execution flow, a flow chart diagram was made and is represented in Figure 4.8. Beginning at the start, the device waits until 2 minutes for a Bluetooth connection. If there is no host ready to connect until time passes, the program goes directly to the autonomous mode explained earlier. In case of there is a host ready to connect with the device the connection is made, and the program continues in a controlled mode by the host. To control the device, the host sends a command that the device, after receiving it, has to identify which command is. If there is the automation command, the program jumps to the autonomous mode to perform the active channels readout. However, if the command is other, the device performs the function. If it is a configuration function, the device will send an OK message to the host, but if it is a reading measurement function, the device will send that results to the host. In both cases, the host can see and analyze the information received in a GUI.

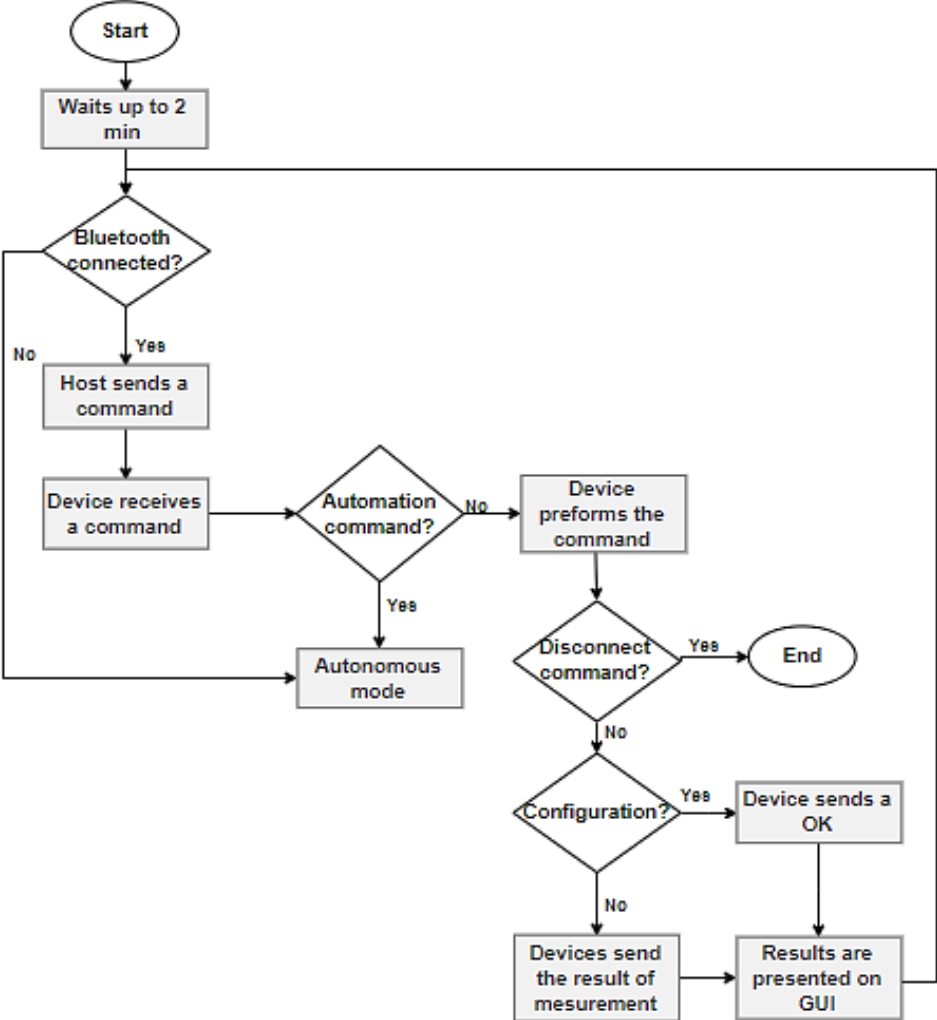


Figure 4.8 - Main execution flow chart.

Chapter 5 - System description and measurements

In this chapter, the final system is characterized, and some results and measurements from it are presented. The idea is to prove that the system works and the ECT is a good method to combine with SHM. To do this it was necessary to build a setup able to keep up the movement of the test structure and analyze the structure failures.

5.1. Setup

As said before, there is a need for a setup capable of following the metallic structure to test. This set up is in Figure 5.1. After the design of the PCB board (A) is complete, the first step is manufacture it. The following phase is to, through the code implemented in the evaluations board used, program the ESP32 soldered in the new PCB and the rest of the board, and also connect a flexible circuit with probes, represented by letter B. The letter C represents the metallic test structure with the faults to identify. The principal perpendicular crack to be detected is represented by letter D and the longitudinal crack to be analyzed is in letter E.

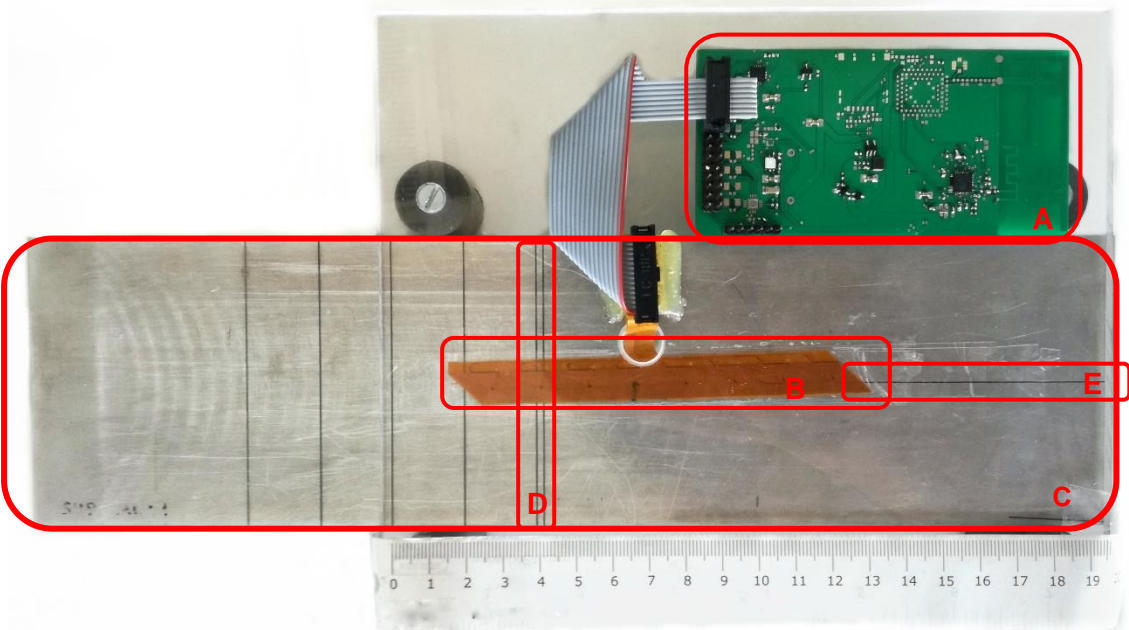


Figure 5.1 - ECT setup.

5.1.1. Probes

To the system being able to be an ECT system, it needs to include an eddy current probe constituted by coils to detect the crack. As seen in Figure 5.1 with the letter B, the probe is a flexible circuit with eight coils disposed horizontally, however only four are used to validate the system. The flexible circuit strip has a 16-pins header terminal to connect with the device, but only the eight central pins are connected to access to the four central coils of the flexible circuit. The flexible circuit probe has 12 cm of length and 1.3 cm of width, and the center of each coil is distanced 1.5 cm of each other.

To discover the value of each coil, it was used the Hioki 3522-50 LCR HiTESTER, that is an LCR meter, connecting the pins of a coil to the instrument. The rounded value of each coil is $4.7\mu H$. Knowing this value and compared with the LDC1614EVM hardware and behavior, it is possible to calculate the value of the parallel capacitor. The value of the coils of LDC1614EVM is rounded to $8\mu H$ and the value of the capacitor is $330pF$, so as the coil used has a value of $4.7\mu H$, the capacitor has to have a value of $3.3nF$ for circuit to resonate around the same frequencies. In Table 5.1, it is represented the value of each coil measured with the developed system, when the probe is over the metallic test structure and when it is in the air (without any conductive material under it).

Table 5.1 - Coils values.

<i>Channel</i>	Coil value in air (μH)	Coil value over conductive material (μH)
<i>Channel 0</i>	4,7176	1,8774
<i>Channel 1</i>	4,8058	1,8504
<i>Channel 2</i>	4,6608	1,7138
<i>Channel 3</i>	4,7571	1,8381

5.1.2. Structure

To start the evaluation of the system it is required a metallic test structure. This structure has 8 cm of width, 30 cm of length and 3.5 cm of height. On the side used to test, it has a crack every 2 cm. To the probe be able to follow the test material it is building an acrylic structure with 20 cm of length and 17 cm of width. To support this acrylic, it is screwed four supports with 3.5 cm of height. Glued in the bottom part of the acrylic is the probe. To be able to the host to has a better notion of distance, the acrylic has a scale.

5.2. Data acquisition

In this section of Chapter 5, a set of results collected with the probe previously described is presented. The configuration used to program the LDC1614 channels was the same in each of them. The reference clock used was the internal one with approximately 43.4 MHz, a deglitch of 3.3 MHz, a *RCOUNT* of 0xFFFF, an *OFFSET* of 0x0000, a *SETTLECOUNT* of 0x0400, a *CLOCK_DIVIDER* of 0x1001 and a *DRIVE_CURRENT* of 8C40.

In Figure 5.2, a set of measurements made over 6 cm, 2 in 2 mm is presented. The probes are in parallel with the test material, being the Channel 0 the first to detect the first crack. The first defect to detect was at 12 mm of the initial position of the setup. The maximum value reached by this channel was $2.1105 \mu H$. Circled in red in Figure 5.2 is the first defect detection of each coil and the value that is measured is legend on top of that. One thing that can be detected is that each channel detects the first defect with a difference of 14 mm of distance. That is, the coils are distanced from each other the 14 mm of distance.

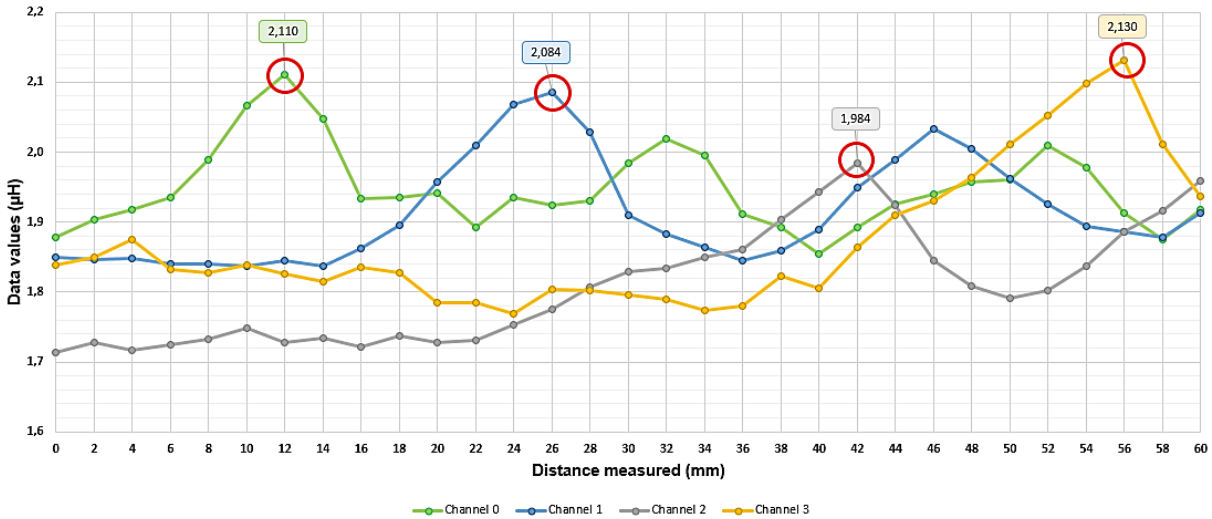


Figure 5.2 - Measurements over distance through four channels, perpendicular cracks.

In Figure 5.3, a single channel acquisition over distance is represented. The channel represented is Channel 0. As it is visible in Figure 5.3, in the distance of 6 cm the Channel 0 can detect three defects, circled in red. The first one is detected at a distance of 12 mm, the second one at a distance of 32 mm, and the final one is detected at 52 cm of distance. What can be taken of this image is that each defect is separated by 20 mm of distance.



Figure 5.3 - Measurements over distance through Channel 0, perpendicular cracks.

In Figure 5.4, a set of measurements made over 6 cm, 2 in 2 mm is presented. The crack testing now is the longitudinal crack, which means that the probe will follow the crack over distance. Similar to the previous evaluation, Channel 0 is the first to detect the defect in the material. Highlighted in red in Figure 5.4, it is represented the distance at each coil detected the defect. Besides detecting the crack, this also shows that the defect is deeper as the distance from the original point increases. It can also measure the length of the defect, being more than 4.6 cm due to the fact that at the final distance the inductance value of the first channel keeps increasing.

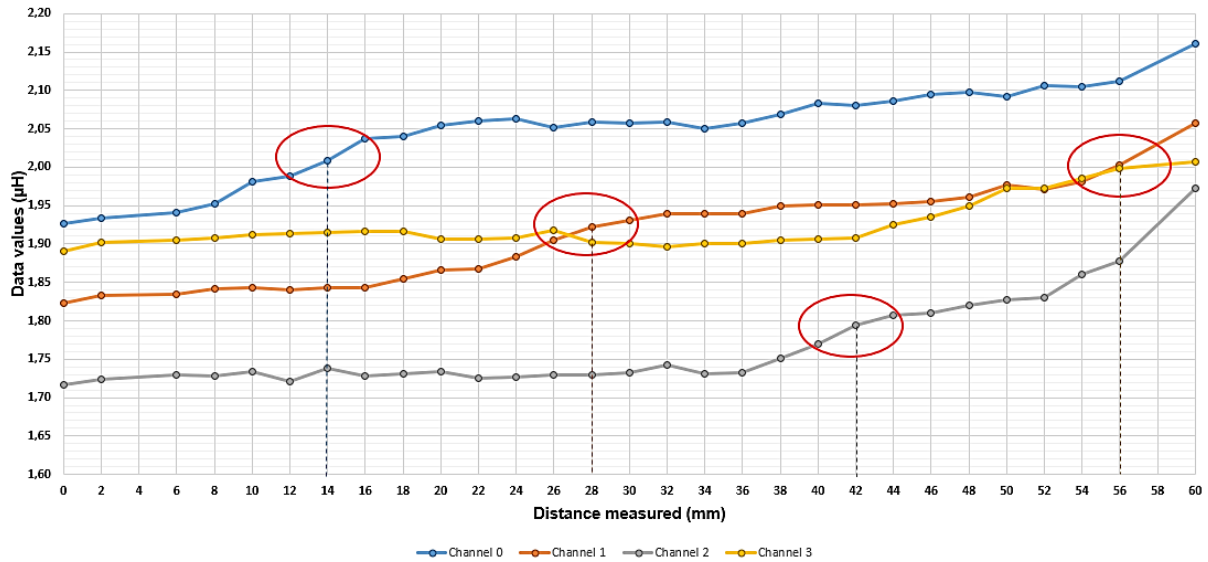


Figure 5.4 - Data acquisition over distance, longitudinal crack.

5.3. Production cost

After the development of the ECT system, it is time to prove that it is a low-cost circuit. In Table 5.2, is present the Mouser Electronics reference of each important chip mentioned and the cost associated with each component, with an estimative value for under than one hundred units. After

analyzing the production cost of the final system, it can be proved that the system is a low-cost production.

Table 5.2 - Production cost.

<i>Quantity</i>	<i>Item</i>	<i>Item reference</i>	<i>Unitary Price (€)</i>	<i>Price (€)</i>
1	Crystal of 26.00 MHz	815-ABM12-116-26T	0,927	0,927
1	ESP32	356-ESP32-D2WD	2,88	2,88
2	LDC1614	595-LDC1614RGHR	5,01	10,02
1	LIS2DE12	511-LIS2DE12TR	1,19	1,19
1	SI7021-A20	634-SI7021-A20-GM	2,75	2,75
1	Others	...	10	10
1	Assembly	...	15	15
1	PCB	...	3	3
			Total:	45,767

Chapter 6 - Conclusion

6.1. Summary and Achievements

In this report an IoT approach for SHM, using eddy current probes to monitor a metallic structure in a real-time operation or in an autonomous operation and permanently mounted, is proposed.

To validate the implemented NDT method, it was elaborated a system composed of a set of four coils, but hardware ready for up eight coils. These probes are placed over the cracks previously identified, to determine the length of a failure that is aligned with the probe. The impedance generated by the coils is converted to digital by the LDC1614 for the rest of the system, and this information is accessed by the ESP32, through an I²C interface. A set of sensors to measure the environment where the device is placed, with the object of better evaluate the damage in the structure. The sensors chosen are an accelerometer, a temperature sensor, and a humidity sensor. Besides the system described there is the possibility of communicating with a host through Bluetooth protocol. A GUI is built to summarize the results, show them to the host, and also control the device.

Although this method already was implemented in some applications, the studies that devote efforts in these combined sets of systems are few and the advantages in terms of effectivity, efficiency and durability are barely studied. Combining IoT with SHM, it brings more assurance in the system itself, having more data to analyze, and more data means more information to make decisions about replacements, improvements or repairs to do in the structure.

Combining all this together, the achieved goals of implementing this device reside on to demonstrate the benefits of using SHM systems to obtain better results in monitoring structures, and in particular metallic structures through the use of NDT especially ECT.

Achieved results of the purposed method were very promising, especially for being effective and having a low cost of production. Multiple measurements were taken to have more results and conclusions about the capabilities of ECT method to analyze a previously detected crack, in a SHM system.

6.2. Future Work

In this sub-section, multiple limitations of the device are addressed, along with a set of enhancements which objective is to repair those limitations and also improve the overall functioning of the system.

- The software is not yet prepared to program multiple LDC1614 to reach more than four coils, which would be one of the next steps as the validation of the system is completed;
- The software is also not ready yet to function in autonomous mode without the host requiring this functionality, and that would be a priority to make it works as the validity of the system is completed;
- Develop firmware for the connection through Wi-Fi or NB-IoT to store the signals on the cloud;
- The device is hardware ready to implement the LPWAN communication, in particular, NB-IoT, to report alarms deliberated by the systems to the cloud, however the chip selected to enable this performance is not fabricated yet and the software programming of this functionality is not developed;
- Demonstrate the benefits of using IoT in a SHM system;
- Characterize the system in electrical terms, that is thermic behavior, aging variations, and power consumption characterization;
- Use the device in a real case of SHM, like to monitor a detected crack from a conductive material bridge.

References

- [1] G. D. M. Willcox, "A brief description of NDT techniques," 2003.
- [2] K. Deutsch, "History of NDT-Instrumentation," Germany, 200.
- [3] S. Osipov, G. Zhang, S. Chakhlov, M. Shtein, A. Shtein, V. Trinh and E. Sirotyan, "Estimation of Parameters of Digital Radiography Systems," in *IEEE Transactions on Nuclear Science, Volume 65*, 2018, pp. 2732-2742.
- [4] L. Zhiyong, Z. Qinlan and L. Xiang, "New Magnetic Particle Cassette NDT Intelligent Detection Device," in *2013 Fourth International Conference on Intelligent Systems Design and Engineering Applications*, Zhangjiajie, China, 2013.
- [5] T. Swait, F. Jones and S. Hayes, "A practical structural health monitoring system for carbon fibre reinforced composite based on electrical resistance," in *Composites Science and Technology*, 2012, pp. 1515-1523.
- [6] Z. Mao, M. Todd and D. Mascareñas, "A haptic-inspired approach of ultrasonic nondestructive damage classification," in *2015 IEEE SENSORS*, Busan, South Korea, 2015.
- [7] Y. Sheiretov, V. Zilberstein and A. Washabaugh, "Surface mounted and scanning periodic field eddy-current sensors for structural health monitoring," in *Aerospace Conference Proceedings*, 2002.
- [8] T. Lüthi, *Non-Destructive*, 2013.
- [9] B. Raj, T. Jayakumar and B. Rao, "Non-Destructive test techniques for assessment of cracks," *Journal of Aero. Soc. of India*, pp. 101-115, August 1994.
- [10] P. Tripler and G. Mosca, *Physics for Scientists and Engineers*, 6th ed., W.H. Freeman and Company, 2008.
- [11] F. Franco, F. Cardoso, L. Rosado, R. Ferreira, S. Cardoso, M. Piedade and P. Freitas, "Advanced NDT Inspection Tools for Titanium Surfaces Based on High-Performance Magnetoresistive Sensors," in *Transactions on Magnetics, vol. 53 n. 4*, IEEE, April 2014, pp. 1-7.

- [12] N. Rodrigues, L. Rosado and P. Ramos, "A Portable Embedded Contactless System for the Measurement of Metallic Material Conductivity and Lift-Off," in *Measurement*, vol. 111, December 2017, pp. 441-450.
- [13] L. Tian, C. Yin, Y. Cheng and L. Bai, "Successive approximation method for the measurement of thickness using pulsed eddy current," in *2015 IEEE International Instrumentation and Measurement Technology Conference (I2MTC) Proceedings*, Pisa, Italy, 2015.
- [14] M. Smetana, T. Strapacova and L. Janoušek, "Pulsed Excitation in Eddy Current Non-Destructive Testing of Conductive Materials," 2008.
- [15] Avanindra, "Multifrequency eddy current signal analysis," Ames, Iowa , 1997.
- [16] L. Shu, H. Songling, Z. Wei and Y. Peng, "Study of pulse eddy current probes detecting cracks extending in all directions," in *Sensor and Actuator A: Physical*, Volume 141, 2007, pp. 13-19.
- [17] A. Mouritz, "Nondestructive inspection and structural health monitoring of aerospace materials," in *Introduction to Aerospace Materials*, 2012, pp. 534-557.
- [18] A. Rerkratn, T. Cheypoca and A. Kaewpoonsuk, "System Development for Tube Inspection Based On Eddy Current Technique," in *SICE Annual Conference 2012*, Akita, Japan, 2012.
- [19] Y. Bihan, F. Loete, J. Ferreira and D. Mencaraglia, "Model-Based Eddy Current Determination of the Electrical Conductivity of Semiconductors," 2016.
- [20] J. Král, R. Smid, H. Ramos and A. Ribeiro, "Thickness Measurement Using Transient Eddy Current Techniques," 2011.
- [21] D. Balageas, C. Fritzan and A. Güemes, *Structural Health Monitoring*, 2006.
- [22] P. Cawley, "Structural health monitoring: Closing the gap between research and industrial deployment," in *Structural Health Monitoring*, 2018, pp. 1225-1244.
- [23] H. Su and K. Chong, "Induction Machine Condition Monitoring Using Neural Network Modeling," in *IEEE Transactions on Industrial Electronics*, Volume: 54 , Issue: 1, IEEE, 2007, pp. 241-249.
- [24] T. Shiotani, D. Aggelis and O. Makishima, "Global Monitoring of Large Concrete Structures Using Acoustic Emission and Ultrasonic Techniques: Case Study," *Journal of Bridge Engineering*, 14(3), pp. 188-192, May 2009.
- [25] P. Wilcox, M. Lowe and P. Cawley, "Omnidirectional guided wave inspection of large metallic plate structures using an EMAT array," in *IEEE Transactions on Ultrasonics, Ferroelectrics, and Frequency Control* (Volume: 52 , Issue: 4), April 2005, pp. 653 - 665.
- [26] Z. Chaudhry, T. Joseph, F. Sun and C. Rogers, "Local-area health monitoring of aircraft via piezoelectric actuator/sensor patches," in *Smart Structures and Materials 1995: Smart Structures and Integrated Systems*, Vol: 2443, 1995, pp. 268-276.

- [27] H. Choi, S. Choi and H. Cha, "Structural Health Monitoring system based on strain gauge enabled wireless sensor nodes," in *5th International Conference on Networked Sensing Systems*, Kanazawa, Japan, 2008.
- [28] F. Rodriguez-Lence, P. Munoz-Esquer, J. Mendez, D. Pardo de Vera and J. Güemes, "Smart sensors for resin flow and composite cure monitoring," in *Proceedings of the 12th International Conference on Composite Materials, ICCM-12*, Paris, France, 1999.
- [29] I. Jamil, M. Abedin, D. Sarker and J. Islam, "Vibration data acquisition and visualization system using MEMS accelerometer," in *International Conference on Electrical Engineering and Information & Communication Technology (ICEEICT)*, page no. 1-6, 2014.
- [30] H. M. Dhivya. A, "Structural health monitoring system-na embedded system approach," *International Journal of Engineering and Technology(IJET)*, vol. 5, pp. 273-281, FEB-March 2013.
- [31] J. I. Baifeng and Q. U. Weilian, "The research of acoustic emission techniques for non destructive testing and health monitoring on civil engineering structures," in *International Conference on Condition Monitoring and Diagnosis*, Beijing, China, 2008.
- [32] G. N. e. al., "Surface mounted periodic field eddy currents sensors for Structural Health Monitoring," in *Proceeding of SPIE*, vol. 4335, 2001, pp. 20-34.
- [33] H. Sodano, "Development of an automated eddy current structural health monitoring technique with an extended sensing region for corrosion detection," in *Struct. Health Monit.*, vol. 6, no. 2, 2007, pp. 111-119.
- [34] B. Diefenderfer, I. Ai-Qad, Y. J., S. Riad and L. A., "Development of a capacitor probe to detect subsurface deterioration in concrete," in *Materials Research Society Symposium Proceedings*, vol. 503, 1998, pp. 231-236.
- [35] W. Shiming, L. Cungang, Z. Zhongmiao and L. Zongliang, "Application of structural health monitoring in Hangzhou Qiantang River tunnel," in *2011 International Conference on Electric Technology and Civil Engineering (ICETCE)*, Lushan, China, 2011.
- [36] J. Wang, L. Tan and C. Yu, "Study on support vector machine in evaluation of bridge structural health monitoring," in *2010 IEEE International Conference on Intelligent Computing and Intelligent Systems*, Xiamen, China, 2010.
- [37] L. Zhang, G. Zhou, Y. Han, H. Lin and Y. Wu, "Application of Internet of Things Technology and Convolutional Neural Network Model in Bridge Crack Detection," in *IEEE Access*, vol. 6, 2018, pp. 39442-39451.
- [38] Y. Sun, Y. Xia, H. Song and R. Bie, "Internet of Things Services for Small Towns," in *International Conference on Identification, Information and Knowledge in the Internet of Things*, 2014.
- [39] S. Jiao, L. Cheng, X. Li, P. Li and H. Ding, "Monitoring fatigue cracks of a metal," *EURASIP Journal on Wireless Communications and Networking*, pp. 1-14, 2016.

- [40] Sensima Inspection, "SHM-EC: Crack monitoring sensor for Structural Health Monitoring," Switzerland, April, 2018.
- [41] M. Nithya, R. Rajaduari, M. Ganesan and K. Anand, "A SURVEY ON STRUCTURAL HEALTH MONITORING BASED ON INTERNET OF THINGS," *International Journal of Pure and Applied Mathematics*, vol. 117, no. 19, pp. 389-393, 2017.
- [42] L. Alonso, J. Barbarán, J. Chen, M. Díaz, L. Llopis and B. Rubio, "Middleware and communication technologies for structural health monitoring of critical infrastructures: A survey," *Computer Standards & Interfaces*, vol. 56, pp. 83-100, 2018.
- [43] F. Pentaris, J. Stonham and J. Makris, "A review of the state-of-the-art of wireless SHM systems and an experimental set-up towards an improved design," in *Eurocon 2013*, Zagreb, Croatia, 2013.
- [44] M. G. Isidori and M. Peralisi, "Design of Wireless Sensor Network for Real-Time," in *IEEE 18th International Symposium on Design and Diagnostics of Electronic Circuits & Systems*, 2015.
- [45] P. Patil and S. Patil, "Review on Structural Health Monitoring," in *International Conference on Electronics, Communication and Aerospace Technology*, 2017.
- [46] T. Das, C. Dutta, A. Kumar and S. Palit, "IN-LINE EDDY CURRENT SMART SENSOR FOR HEALTH MONITORING OF HIGH SPEED DRAWN WIRES," in *International Symposium on Structural Health Monitoring and Nondestructive Testing*, Saarbruecken, Germany, 4-5 Oct. 2018.
- [47] Espressif Systems, "ESP32 Series Datasheet," 2018.
- [48] Silicon Laboratories, "Si7021-A20 DataSheet," 2016.
- [49] ST Microelectronic, "LIS2DE12 DataSheet," 2017.
- [50] Texas Instruments, "LDC1612, LDC1614 Multi-Channel 28-Bit Inductance to Digital Converter (LDC) for Inductive Sensing," 2014.
- [51] Texas Instruments, [Online]. Available: <http://www.ti.com/tool/LDC1614EVM#descriptionArea>. [Accessed 04 January 2019].
- [52] J. Ihm, F. Chang, J. Huang and M. Derriso, "Diagnostic Imaging Technique for Structural Health Monitoring," in *Proc. 2nd European Workshop "Structural Health Monitoring 2004"*, Munich, Germany, July, 7-9, 2004, pp. 109-116.
- [53] R. Prabhakaran, "Damage assessment through electrical resistance measurement in graphite fiber-reinforced composites," in *Experimental Techniques*, vol. 14, no. 1, 1990, pp. 16-20.
- [54] S. Kessler, "Piezoelectric Based In-Situ Damage Detection of Composite Materials for Structural Health Monitoring Systems," PhD Dissertation, MIT, Massachusetts, 2002.
- [55] Telit, "ME310G1," 2019.

Appendix I - Commands definition

<i>Command name</i>	<i>Function</i>	<i>Button</i>	<i>Value</i>	<i>Size</i>	<i>Data</i>			<i>Direction</i>
<i>OK acknowledge</i>	0x01		1	0	NULL			Device to Host
<i>NOK acknowledge</i>	0x01		0	0	NULL			Device to Host
<i>Reset</i>	0x00	RESET LDC	1	0	NULL			Host to Device
<i>Load</i>	0x10	LOAD	1	0	NULL			Host to Device
<i>Store</i>	0x11	STORE	<i>Channel</i>	8*4	<i>LDC_Config</i>			Host to Device
<i>Read temperature</i>	0x20	READ ENVIRONMENT	1	0	NULL			Host to Device
	0x20		Temperature [°C]	0	NULL			Device to Host
<i>Read humidity</i>	0x21		1	0	NULL			Host to Device
	0x21		Humidity [%]	0	NULL			Device to Host
<i>Read acceleration</i>	0x22		1	0	NULL			Host to Device
	0x22		1	3*4	X [m/s ²]	Y [m/s ²]	Z [m/s ²]	Device to Host

<i>Read frontend channels</i>	0x60	READ/START	Channel	0	NULL	Host to Device
	0x60		Channel	0	NULL	Device to Host
<i>Switch frontend reference clock</i>	0x63	PROGRAM	INT = 7169 EXT = 7681	0	NULL	Host to Device
<i>Change frontend input deglitch</i>	0x64		1 MHz = 33289 3.3 MHz = 33292 10 MHz = 33293 33 MHz = 3329	0	NULL	Host to Device
<i>Change frontend conversion time</i>	0x65		Channel	4	RCOUNT	Host to Device
<i>Change frontend conversion offset</i>	0x66		Channel	4	OFFSET	Host to Device
<i>Change frontend settling time</i>	0x67		Channel	4	SETTLECOUNT	Host to Device
<i>Change frontend reference clock divider</i>	0x68		Channel	4	CLOCK_DIVIDER	Host to Device
<i>Change frontend current drive level</i>	0x69		Channel	4	DRIVE_CURRENT	Host to Device
<i>Automation</i>	0x70	AUTOMATION	1	0	NULL	Host to Device
<i>Disconnect</i>	0x30	DISCONNECT	1	0	NULL	Host to Device

Appendix II – PCB design

